

IDENTIFICATION AND CHARACTERIZATION OF MUTATIONS IN THE
DROSOPHILA MITOCHONDRIAL TRANSLATION ELONGATION FACTOR
ICONOCLAST

by

Catherine F. Trivigno

A Dissertation Submitted to the Faculty of
The Charles E. Schmidt College of Science
in Partial Fulfillment of the Requirements for the Degree of
Doctor of Philosophy

Florida Atlantic University

Boca Raton, FL

August 2010


IDENTIFICATION AND CHARACTERIZATION OF MUTATIONS IN THE
DROSOPHILA MITOCHONDRIAL TRANSLATION ELONGATION FACTOR
ICONOCLAST

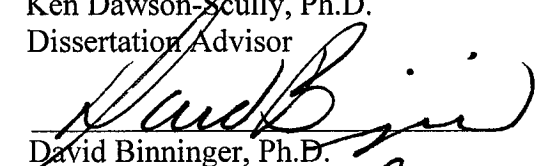
by

Catherine Trivigno


This dissertation was prepared under the direction of the candidate's dissertation advisor, Dr. Ken Dawson-Scully, Department of Biological Sciences, and has been approved by the members of her supervisory committee. It was submitted to the faculty of the Charles E. Schmidt College of Science and was accepted in partial fulfillment of the requirements for the degree of Doctor of Philosophy.

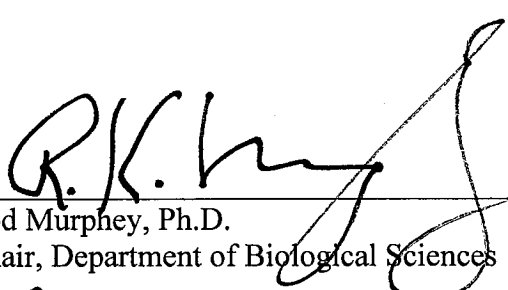
SUPERVISORY COMMITTEE:

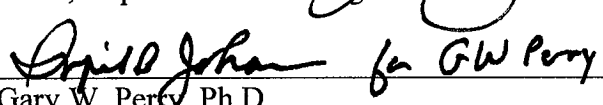

Ken Dawson-Scully, Ph.D.
Dissertation Advisor

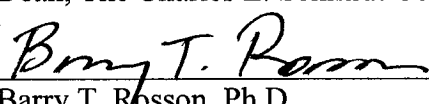

David Binner, Ph.D.


Zhongwei Li, Ph.D.


Herbert Weisbach, Ph.D.


Rod Murphey, Ph.D.
Chair, Department of Biological Sciences


Gary W. Perry, Ph.D.
Dean, The Charles E. Schmidt College of Science


Barry T. Rosson, Ph.D.
Dean, Graduate College

July 13, 2010
Date

ACKNOWLEDGEMENTS

I am forever grateful to the many people and organizations whose support made this work possible, especially Dr. Herb Weissbach, Dr. Zhongwei Li, Dr. David Binniger, Dr. Rod Murphey, Dr. Theodor Haerry, and my advisor, Dr. Ken Dawson-Scully. Special thanks go to Dr. Tanja Godenschwege, Sharon, David, Roger, Jeremy, and the fly lab grad students. Thanks also to Steve for always being there for me, rain (and there was a lot of it) or shine. I am especially grateful to The FAU Foundation and the Graduate College as well as Karen Fisher and Julia Lampman. Thank you to The National Institutes of Health, the National Science Foundation, the Mc Guinty Foundation, the Genetics Society of America, the Executive Women of the Palm Beaches, Phi Kappa Phi National Honor Society, and Cold Spring Harbor Laboratories for funding my work and conference participation. Finally, I would like to thank my family for their support and for believing in me and my dream, especially mom, John, Marie, and Joe, and most of all Angela.

ABSTRACT

Author: Catherine F. Trivigno

Title: Identification and Characterization of Mutations in the *Drosophila* Mitochondrial Translation Elongation Factor Iconoclast

Institution: Florida Atlantic University

Dissertation Advisor: Dr. Kenneth Dawson-Scully

Degree: Doctor of Philosophy

Year: 2010

Mitochondrial disorders resulting from defects in oxidative phosphorylation are the most common form of inherited metabolic disease. Mutations in the human mitochondrial translation elongation factor *GFMI* have recently been shown to cause the lethal pediatric disorder Combined Oxidative Phosphorylation Deficiency Syndrome (COXPD1). Children harboring mutations in *GFMI* exhibit severe developmental, metabolic and neurological abnormalities. This work describes the identification and extensive characterization of the first known mutations in *iconoclast* (*ico*), the *Drosophila* orthologue of *GFMI*. Expression of human *GFMI* can rescue *ico* null mutants, demonstrating functional conservation between the human and fly proteins. While point mutations in *ico* result in developmental defects and death during embryogenesis, animals null for *ico* survive until the second or third instar larval stage. These results indicate that in addition to loss-of-function consequences, point mutations

in *ico* appear to produce toxic proteins with antimorphic or neomorphic effects.

Consistent with this hypothesis, transgenic expression of a mutant ICO protein is lethal when expressed during development and inhibits growth when expressed in wing discs. In addition, animals with a single copy of an *ico* point mutation are more sensitive to acute hyperthermic or hypoxic stress. Removal of the positively-charged tail of the protein abolishes the toxic effects of mutant ICO, demonstrating that this domain is necessary for the harmful gain-of-function phenotypes observed in *ico* point mutants. Further, expression of GFP-tagged constructs indicates that the C-terminal tail enhances ectopic nuclear localization of mutant ICO, suggesting that mislocalization of the protein may play a role in the antimorphic effects of mutant ICO. Taken together, these results illustrate that in addition to loss-of-function effects, gain-of-function effects can contribute significantly to the pathology caused by mutations in mitochondrial translation elongation factors.

IDENTIFICATION AND CHARACTERIZATION OF MUTATIONS IN THE
DROSOPHILA MITOCHONDRIAL TRANSLATION ELONGATION FACTOR
 ICONOCLAST

List of Figures.....	x
List of Tables	xii
Chapter 1. Introduction and Statement of Purpose.....	1
Introduction	1
Mitochondrial Biogenesis.....	1
Comparison of GFM1 and GFM2	2
Mutations in GFM1 and Human Disease	4
<i>Drosophila</i> as a Model Organism - History and Overview.....	8
Life Cycle of <i>Drosophila</i>	10
UAS-GAL4 System.....	10
Statement of Purpose.....	11
Chapter 2. Materials and Methods.....	18
Fly Strains.....	18
<i>ico</i> Point Mutant Lines	18
Generation of <i>ico</i> Deletion Mutants	18
Isogenization of Fly Lines	19

UAS-GAL4 Drivers.....	19
RNAi Transgenic Flies	19
Mapping of <i>ico</i>	20
Sequencing of <i>ico</i> missense alleles.....	21
Bioinformatics	21
Molecular Biology.....	21
Genetics	22
Enhancer and Suppressor Screens for Interactions with TGF-beta	
Signaling.....	22
Clonal Analysis of <i>ico</i> Alleles in the Eye.....	23
Behavioral Assays	23
Hyperthermia.....	23
Anoxia	24
Accession Numbers	24
Chapter 3. Identification and Cloning of <i>iconoclast</i>	25
Introduction	25
Results	26
Mapping of <i>iconoclast</i>	26
Confirmation That <i>ico</i> Is CG4567	28
Sequence and Functional Conservation of ICO and Human GFM1	30
Investigation of Conservation of Function between ICO with CG31159, The	
Fly GFM2 Othologue	31
Deletion of the C-terminal Tail of ICO and Rescue of <i>ico</i> Mutations	32

Discussion.....	32
Chapter 4. Developmental Phenotypes of <i>ico</i> Mutants	38
Introduction	38
Recessive Lethality of <i>ico</i> Mutations	38
Phenotypes of Heterozygous <i>ico</i> Mutants	39
RNAi Loss-of-Function Phenotypes	39
Effects of <i>ico</i> Mutations on Somatic Cells	40
Discussion.....	42
Chapter 5. Effects and Subcellular Localization of Mutant ICO Proteins	44
Introduction	44
Results	44
Harmful Effects of ICO ^{II032} Expression.....	44
Contribution of the C-terminal Tail to Toxic Effects of ICO ^{II032}	45
Role of the C-terminal Tail in Localization of Mutant ICO.....	46
Functional Rescue by Mutant Human GFM1 Proteins	48
Discussion.....	49
Chapter 6. Effects of <i>ico</i> on Response to Acute Stress	55
Introduction	55
Results	56
Effects of <i>ico</i> Mutations on Response to Hyperthermic Insult.....	56
Effects of <i>ico</i> Mutations on Response to Anoxic Insult	57
Preliminary Studies of the Effects of <i>ico</i> Knockdown on Response to	
Hyperthermic and Anoxic Insult	58

Discussion.....	59
Chapter 7. Discussion and Future Directions	68
Introduction	68
Cloning and of <i>iconoclast</i> and Characterization of Mutations.....	68
Developmental Phenotypes of <i>ico</i> Mutations.....	68
Effects of Acute Stress on <i>ico</i> Heterozygotes	69
Toxic Effects of Mutant ICO Proteins.....	70
Role of the C-terminal Tail of ICO	71
Functionality of Mutant Human GFM1	72
Summary.....	74
Functionality of Mutant Human GFM1	72
References	76

LIST OF FIGURES

Figure 1.1. The Mitochondrial Oxidative Phosphorylation System.....	13
Figure 1.2. Translation Elongation.....	14
Figure 1.3. Ribbon Structures of GFM1 (A) and GFM2 (B)	15
Figure 1.4. The Life Cycle of <i>Drosophila</i>	16
Figure 1.5. The <i>Drosophila</i> UAS-GAL4 System.....	17
Figure 3.1. Candidate Genes and P-element Transposons	34
Figure 3.2. Alleles of <i>iconoclast</i>	34
Figure 3.3. Sequence Alignment of ICO and Human GFM1	35
Figure 4.1. Clonal Analysis of <i>ico</i> Mutants in the Eye	43
Figure 5.1. Expression of Mutant Forms of ICO Reduces Growth and Affects Patterning in Wings	52
Figure 5.2. Effects of the C-terminal Tail on Subcellular Localization of ICO Proteins	53
Figure 5.3. Summary of Functional Rescue Results	54
Figure 6.1. Behavioral Assays.....	61
Figure 6.2. Example of Disparate Sensitivity to Hyperthermia – The Effects of Heat Shock on Failure and Recovery Times.....	62
Figure 6.3. Effect of <i>ico</i> Mutations on the Time to Failure and Recovery from Hyperthermia	64

Figure 6.4. Effect of <i>ico</i> Alleles on Time to Recover from Anoxia.....	66
Figure 6.5. Preliminary Results of <i>ico</i> Knockdown Animals in the Anoxia Assay	67
Figure 7.1. JC-1 Staining in the Fly Neuromuscular Junction	75

LIST OF TABLES

Table 3.1. Comparison of Identity of Protein Sequences of ICO and GFM1

Orthologues in Other Species	37
------------------------------------	----

CHAPTER 1

INTRODUCTION AND STATEMENT OF PURPOSE

INTRODUCTION

Mitochondrial Biogenesis

The mitochondrial Oxidative Phosphorylation (OXPHOS) system is located in the inner mitochondrial membrane and supplies approximately 90% of the energy used by eukaryotic cells (Schapira, 2006). The OXPHOS system is comprised of the mitochondrial respiratory chain (complexes I-IV) and complex V, ATP synthase (FIG. 1.1). While all five complexes contain proteins that are encoded by nuclear genes, complexes I, III, IV, and V also contain a total of thirteen proteins encoded by mitochondrial DNA (mtDNA) (Anderson et al., 1981). The synthesis of these thirteen mitochondrial proteins requires a host of nuclear-encoded factors. These factors, which are translated in the cytoplasm and transported into the mitochondria, include two initiation factors, three sets of elongation factors, a release factor and a recycling factor (Gao et al., 2001; Hammarsund et al., 2001; Koc & Spremulli, 2002; Ling et al., 1997; Ma, Farwell, Burkhardt, & Spremulli, 1995; Woriak, Burkhardt, & Spremulli, 1995; Xin, Woriak, Burkhardt, & Spremulli, 1995; Zhang & Spremulli, 1998).

As in cytoplasmic translation, protein biosynthesis in mitochondria takes place in three phases: initiation, elongation, and termination. The elongation phase is considered to be one of the most highly conserved processes in living organisms

(Gao et al., 2001). In addition to tRNAs and rRNAs which are encoded by mitochondrial DNA, the elongation step requires three sets of nuclear encoded elongation factors. The first, EF-Tu, is a GTPase that delivers the correct aminoacyl tRNA to the acceptor site (A site) on the ribosome. The second factor, EF-Ts, “recharges” the EF-Tu by exchanging GTP for GDP. Following peptide bond formation, the third set of factors, GFM1 and GFM2 (also known as EFG1 and EFG2), is believed to be responsible for catalyzing the translocation of the peptidyl-tRNA from the A site to the peptidyl site (P site, FIG 1.2), allowing the next t-RNA to interact with the A site (reviewed in Gao et al., 2001).

Comparison of GFM1 and GFM2

It is unknown why eukaryotic genomes each contain two genes encoding distinct but highly conserved mitochondrial GFM proteins (Gao et al., 2001; Hammarsund et al., 2001). The sequence and structure of both GFM proteins are similar, with the most striking difference being the short, positively charged C-terminal “tail” of GFM1 (FIG 1.3). The conservation of both genes in organisms ranging from yeast to humans indicates that, while the two proteins appear alike in many ways, their functions may not be completely redundant.

Recent research has supported this hypothesis. For example, it has been demonstrated that amino acid misincorporation and respiratory chain assembly defects in human caused by MELAS mutations in human myoblasts can be partially repressed by overexpression of GFM2, but not GFM1, suggesting that GFM2 may play a role in mitochondrial translation elongation quality control (Sasarman, Antonicka, & Shoubridge, 2008).

In addition, another recent paper, published after the research described in this dissertation was completed, demonstrated that GFM2, but not GFM1, is necessary for recycling of ribosomes during translation (Tsuboi et al., 2009). Tsuboi et al. also demonstrated that while human GFM1 did exhibit robust translation elongation activity in their *in vitro* experiment, GFM2 showed minimal translation elongation activity. They propose that the translation elongation and ribosome recycling roles played by bacterial EFG have been split between GFM1 and GFM2 in mitochondria, and that GFM2 should instead be termed a recycling factor. Only one GFM2 isoform was tested by this group, so it is unknown whether the other isoforms retain significant translation elongation factor activity.

Additional research also suggests that GFM1 has an additional, crucial function that does not overlap that of GFM2. For example, mutations in *Mef1*, the yeast orthologue of *GFM1*, result in a *petite* phenotype and reduced mitochondrial protein synthesis, in contrast to mutations in the yeast *GFM2* orthologue, *Mef2*, which do not produce a respiratory phenotype (Myers, Pape, & Tzagoloff, 1985; Vambutas, Ackerman, & Tzagoloff, 1991). In *C. elegans*, RNAi knockdown of *F29C12.4*, the worm orthologue of *GFM1*, results in slow growth, embryonic lethality, early larval arrest, and maternal sterility, depending on the RNAi construct used (www.wormbase.org, release WS200, March 2009), while no phenotypes are associated with knockdown of *Y119D3B.14*, the worm *GFM2* orthologue (www.wormbase.org, release WS200, March 2009). In addition, it has been shown that OXPHOS pathway function is severely curtailed in homozygous *GFM1*- human fibroblasts, even though GFM2 is present (Coenen et al., 2004). It was also demonstrated that while the activity

of the OXPHOS pathway can be partially restored in these cells by expression of a wild-type *GFM1* transgene, overexpression of a wild-type *GFM2* transgene does not rescue the dysfunctional pathway, indicating that the loss of mitochondrial translational competence in *GFM1*- cells is not solely due to reduced levels of translation factors (Coenen et al., 2004). These data suggest that GFM1 may play an additional, unknown role that is not shared by GFM2.

Mutations in GFM1 and Human Disease

Mitochondrial disorders resulting from OXPHOS defects are the most common inherited metabolic disease, occurring in approximately 1:5,000 births worldwide (Thorburn, 2004). For years, it was assumed that mutations in mtDNA were the underlying cause of most of these defects, and research efforts focused on the identification and characterization of such mutations, as reviewed by Jacobs (Jacobs, 2003). However, a large proportion of cases of OXPHOS deficiency appear to be inherited in an autosomal recessive fashion, with no defects found in the mtDNA of these patients, implying that mutations in nuclear encoded genes are responsible for some of these disorders (Jacobs & Turnbull, 2005). Until recently, if a patient with a mitochondrial disorder did not display any mutations in their mtDNA, and the defect was assumed to be nuclear, little or no effort was taken to identify the affected gene. It has become increasingly evident, however, that mutations in nuclear-encoded mitochondrial components are strongly predictive of a more severe clinical course than that caused by most mtDNA mutations (Rubio-Gozalbo et al., 2000). Patients with such nuclear mutations tend to present with symptoms much earlier, often in very early childhood, followed by severe, rapidly progressing metabolic disturbances and

developmental decline, often culminating in death before the age of ten (Rubio-Gozalbo et al., 2000). These clinical observations, as well as the development of improved genetic screening technologies, have led to an increased effort to identify and characterize nuclear mutations that underlie mitochondrial dysfunction.

In 2004, the first mutation in *GFM1* was identified in a sister and brother born to consanguineous parents (Coenen et al., 2004). The index patient displayed intrauterine growth retardation, and at birth she presented with mild microcephaly, rigidity, and lack of spontaneous movements. By day twelve, she demonstrated profound OXPHOS defects, metabolic acidosis and liver failure, followed by death at day 27. An autopsy revealed extensive liver necrosis as well as a small corpus callosum and cystic lesions in the brain. Interestingly, her heart and skeletal muscles appeared normal. Her brother demonstrated severely delayed development and presented with generalized brain atrophy and liver failure at 7 weeks, followed by death at the age of 5 months. Although his brain and liver were severely impacted, his heart, like his sister's, appeared normal. No mutations were found in the mtDNA of either patient. Significantly, these patients had Combined Oxidative Phosphorylation Deficiency (COXPD), which is defined as a severe reduction in the assembly of the respiratory chain complexes I, III, IV, and V, and suggests a defect in mitochondrial translation. The sequences of several nuclear genes known to play a role in mitochondrial biogenesis were therefore examined, and both patients were shown to be homozygous for an N174S mutation in *GFM1*. Cultured fibroblasts from both patients revealed significant defects in OXPHOS. While overexpression of transgenic *GFM1* was able to rescue the OXPHOS defect in these fibroblasts, overexpression of *GFM2* had little

effect, suggesting that the loss of OXPHOS competency in these mitochondria was not solely due to reduced levels of GFM proteins and that the roles of GFM1 and GFM2 are not completely redundant.

Soon after, another pair of siblings with mutations in GFM1 was identified (Antonicka, Sasarman, Kennaway, & Shoubridge, 2006). Both exhibited reduced intrauterine growth. Like the previous patients, the first sibling presented with severe metabolic disorders and liver dysfunction, and she died at 9 days of a pulmonary hemorrhage following respiratory insufficiency. Microcephaly and extensive liver damage were present, but the heart appeared normal, and while the skeletal muscle showed reduced cytochrome C oxidase activity, no ragged red fibers or inclusions were noted. Interestingly, while no significant amounts of GFM1 were found in mitochondria from the patient's muscle, liver, or fibroblasts, GFM1 was present in mitochondria from heart tissue. At 24 weeks of gestation, her sibling demonstrated marked growth retardation upon ultrasound examination, and a decision was made to induce birth. The infant died within 45 minutes of birth. Intriguingly, although cultured fibroblasts from both patients showed the same pattern of OXPHOS defects, autopsy of the second patient revealed no diagnostic abnormalities in any of her organs, with the exception of mild iron staining in the liver. Both patients were found to be heterozygous for two mutations in GFM1: S321P as well as a deletion that results in a STOP codon at position 607.

In 2007, an additional patient with two novel mutations in GFM1 was identified (Valente et al., 2007). One week after birth, she was evaluated for dysmorphic signs (flattened nasal bridge, small hands and feet, low-set ears, and short tibias). Brain

ultrasound and ECG were normal at this time. At 3 weeks, the patient started having feeding difficulties and weight loss. At three months neurological examination revealed a paucity of spontaneous movements and reduced muscle tone, and an EEG showed global, severe disorganization. At 5 months she presented with frequent bouts of vomiting as well as significantly elevated serum lactate and pyruvate, indicating a significant loss of OXPHOS competency. Brain MRI indicated extensive abnormalities normally associated with the mitochondrial disorder Leigh's Disease. In addition to the OXPHOS deficiency, at age 14 months the patient had microcephalia, severely delayed motor and mental development, as well as muscle tone and reflex defects, and she died of respiratory insufficiency at age 16 months. Interestingly, unlike the other patients, who exhibited significant liver damage, no hepatopathy was found in this patient.

It is interesting to note the tissue specificity of the deleterious effects of GFM1 mutations. In each of the above patients, the brain, and in most cases the liver, are severely affected by GFM1 mutations, while the heart, also an organ that consumes a great deal of energy, does not appear to be significantly affected. While no detectable levels of GFM1 were present in the liver mitochondria of these patients, a significant amount (60% of control) of GFM1 was found in mitochondria in the heart (Antonicka et al., 2006). Antonicka et al. postulate that the harmful effects of GFM1 mutations may be due to loss-of-function consequences and that perhaps mutant GFM1 protein is less stable in some tissues than in others, but the reasons for this disparity are unclear.

When developing therapeutic strategies for treating the symptoms of patients with mutations in *GFM1*, it will be important to understand the mechanisms whereby mutations in this gene cause disease as well as why certain tissues may be more

susceptible to these harmful effects. An animal model system would be useful for investigating these issues.

***Drosophila* as a Model Organism - History and Overview**

For more than 100 years, the fruit fly *Drosophila melanogaster* has played a critical role in biological research. In the early 1900's, Morgan, Sturtevant, Bridges, and Muller used this model organism to investigate the nuances of Mendelian heredity (Muller, 1928; Sturtevant, Bridges, & Morgan, 1919). Lewis used the fly to elucidate gene structure in the 1950's and won the Nobel prize for his work on homeotic gene complexes (Lewis, 1941, 1945, 1948, 1952, 1978, 1982). In the 1970's, Benzer's pioneering research established *Drosophila* as a powerful model to investigate the genetic basis of behavior (Konopka & Benzer, 1971). In the 1980's, Wieschaus and Nusslein-Volhard used large-scale mutagenesis screens to identify several genes that play key roles in development (Nüsslein-Volhard, E., & H., 1984). More recently, the fly has also been used successfully as a model system to study the underlying mechanisms of a range of human diseases, including neurodegenerative disorders such as Parkinson's Disease (Feany & Bender, 2000; Haywood & Staveley, 2006; Scherzer, Jensen, Gullans, & Feany, 2003) and Huntington's Disease (Jackson et al., 1998; Ravikumar et al., 2004), metabolic and mitochondrial disorders (Baker & Thummel, 2007; Bier, 2005; Lazzaro & Galac, 2006; Luong et al., 2006; Milne et al., 2007; Tickoo & Russell, 2002; Zhou et al., 2008) as well as to screen for therapeutic strategies to treat these diseases.

There are many characteristics that make *Drosophila* an attractive model system for biological and biomedical research. In addition to the benefits afforded by the small

size of the fly, its sequenced genome, and its rapid life cycle (which is described below), the large *Drosophila* research community has developed a great variety of resources and tools. Tens of thousands of fly strains have been created, characterized, and catalogued, and many are readily available from repositories such as the Bloomington Drosophila Stock Center. In addition to mutations in individual genes, stocks with deficiencies (which are useful for mapping and complementation testing), transposons (useful for mutagenesis), or transgenic constructs, including those for RNAi expression, are available. *Flybase* (www.flybase.org) is a comprehensive resource that provides a wealth of cross-referenced information about genes, protocols, reagents, and publications.

In addition to the tractability of the fly and the ready availability of stocks, reagents, and genetic tools, the high degree of conservation of molecular mechanisms between flies and vertebrates, including humans, makes the fly an appealing and relevant model system. In fact, it is estimated that more than 60 percent of human genes have conserved functional fly orthologues (Bernards & Hariharan, 2001). Duplication of several genes has occurred over time in vertebrates (Wang & Gu, 2000), often making complete knockout of function difficult. This is not the case in *Drosophila*, which has a compact genome of about 14,000 genes (Celniker & Rubin, 2003). This attribute, combined with a variety of *Drosophila* mutagenesis techniques as well as the relative ease of generation of transgenic animals, make the fly a useful system for studying the consequences of both loss-of-function and gain-of-function mutations.

Life Cycle of *Drosophila*

The reproductive cycle of *Drosophila* takes about 12 days at 25°C, reviewed in (Nichols, 2006). After 21-24 hours of embryonic development, eggs hatch and first instar larvae emerge. During the next 48 hours, two more molts occur, producing second and third instar larvae. After two days, the third instar larvae crawl out of the food, attach themselves to a solid substrate, and undergo metamorphosis as pupae for the next 5-7 days. After metamorphosis, the adult emerges from the pupal case in a process called eclosion, and the cycle begins anew. A single female can lay hundreds of eggs in less than one week, producing large numbers of progeny in a short period of time.

Because of this short generation period, genetic crosses can be performed very quickly. As a result, complex genetic screens or sets of crosses involving multiple generations of animals, which would be cumbersome in many other model organisms, can be performed easily in a few weeks or months in *Drosophila*. The small size of this organism and the facility with which large numbers of progeny can be produced and maintained also makes the fly an ideal model system to use for large-scale screens and experiments. In addition, each of the developmental stages of the fly (embryo, larva, pupa, and adult) are well-characterized, and each has been used successfully for different types of studies (Nichols, 2006).

UAS-GAL4 System

The UAS-GAL4 expression system has been called the “fly geneticist’s Swiss Army Knife” (Duffy, 2002). Brand and Perrimon developed this system (FIG 1.4) to allow controlled expression of transgenic constructs (Brand & Perrimon, 1993). The *S.*

cerevisiae transcription factor GAL4 regulates expression of genes through DNA binding at a series of four similar, 17-base pair sites which serve as an enhancer element and are collectively known as *Upstream Activating Sequences* (UAS). Both GAL4 and the *UAS* are specific to yeast and are not found in wild-type *Drosophila*. However, constructs in which a gene of interest is cloned downstream of a *UAS* element may be microinjected into fly embryos to create a fly line with a stably integrated transgene that can be expressed under the control of the *UAS*. This transgenic fly strain can then be crossed to a “driver” strain that expresses transgenic GAL4 under the control of tissue-specific regulatory sequences. The GAL4 thus expressed will in turn drive the tissue- and temporal-specific expression of the *UAS* target construct in the progeny. A large number of well-characterized driver lines are available from the Bloomington *Drosophila* Stock Center, making it relatively easy to selectively express transgenes in a wide variety of tissues and temporal patterns.

Further temporal control of expression can be achieved by using the GAL4 inhibitor GAL80. At lower temperatures (18-20C), GAL80 binds to GAL4 and prevents GAL4-induced transcriptional activation (Ma & Ptashne, 1987). When the flies are shifted to 25C (the “permissive temperature”), GAL80 no longer associates with the GAL4, and the target transgene is expressed. This modification of the UAS-GAL4 system is especially useful when expressing RNAi constructs or transgenes that can cause lethality during development.

STATEMENT OF PURPOSE

Mitochondrial diseases caused by OXPHOS deficiencies are very common. It is becoming increasingly clear that mutations in nuclear-encoded mitochondrial proteins

are responsible for a large proportion of cases of oxidative phosphorylation deficiency (11). While relatively few mutations in genes involved in mitochondrial biogenesis have been reported, a concerted effort has only recently begun to identify the nuclear mutations that underlie many cases, and it is likely that many more will be discovered in the near future. Characterization and of several of the relevant nuclear mutations that have been identified, such as those in *GFMI*, has only just begun.

When developing therapeutic strategies for treating the symptoms of patients with mutations in *GFMI*, it will be important to understand how these mutations cause disease as well as the underlying mechanisms that make certain tissues more susceptible to the deleterious effects of these mutations. An animal model system would be useful for characterizing the effects of *GFMI* mutations. With this in mind, this project addressed the following specific aims:

1. Identification of mutations in and cloning of *iconoclast* (*ico*), the fly orthologue of *GFMI*, and confirmation of functional conservation between the fly and human proteins.
2. Characterization of the developmental phenotypes of *ico* missense and deletion mutations.
3. Investigation of gain-of-function and antimorphic effects of mutant ICO proteins.
4. Examination of the response of heterozygous *ico* mutants to acute stress.

The results of these experiments have established a *Drosophila* model system to examine the deleterious effects of mutation in mitochondrial translation elongation

factor G1 and have increased our understanding of the mechanisms underlying these defects.

Figure 1.1 The Mitochondrial Oxidative Phosphorylation System. The mitochondrial oxidative phosphorylation (OXPHOS) system is comprised of the mitochondrial respiratory chain (complexes I-IV) and complex V, ATP synthase. Each complex is made up of several subunits. As shown below the illustration, all five complexes contain components encoded by nuclear genes. Each of the complexes, except Complex II, also contains at least one subunit encoded by a mitochondrial gene. Disruption of mitochondrial translation, therefore, can negatively affect the assembly of Complexes I, III, IV, and V. Adapted from (Bellance, Lestienne, & Rossignol, 2009).

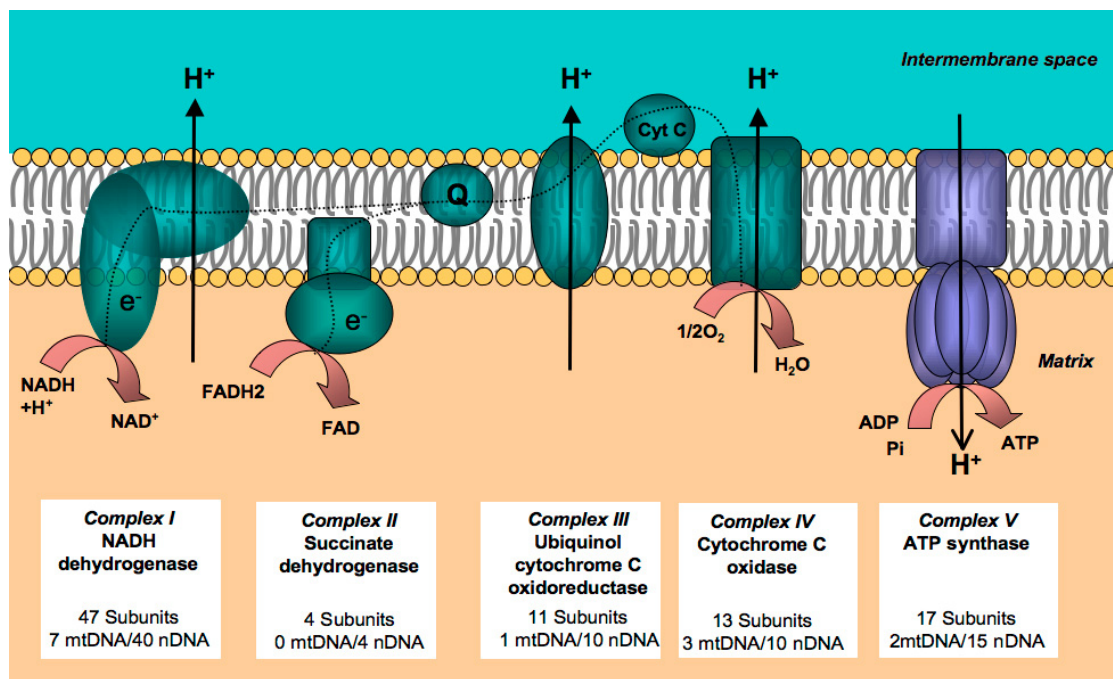
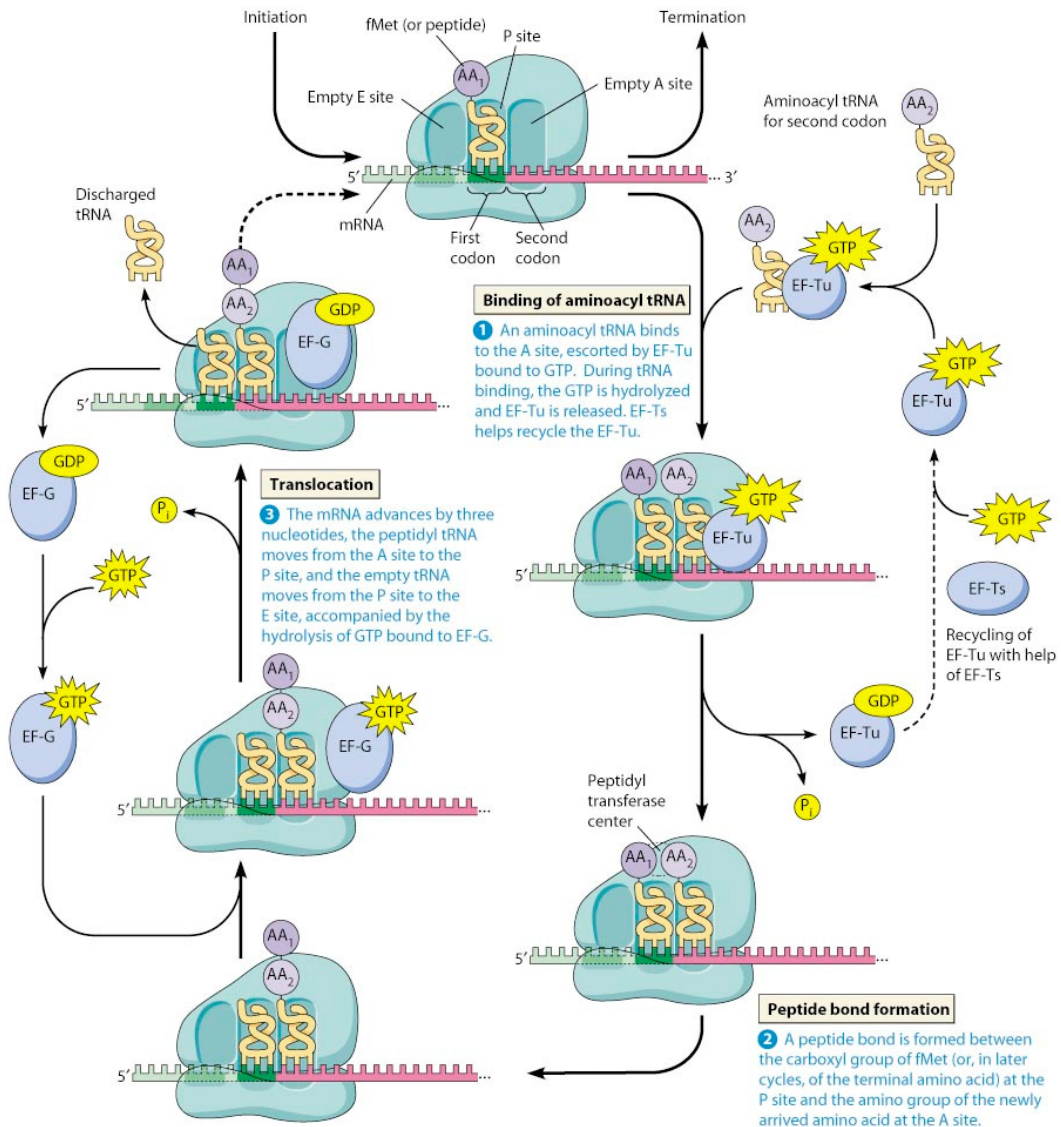


Figure 1.2 Translation Elongation. GFM proteins (here shown as “EF-G”) allow the tRNA to move from the A site to the P site along the ribosome during translation (from Pearson Education Inc., 2009)



Copyright © 2009 Pearson Education, Inc.

Figure 1.3 Ribbon structures of GFM1 (A) and GFM2 (B). In addition to their sequence similarity, the structures of the two GFM proteins are very similar. Note the barrel-shaped mitochondrial targeting sequence (in red) at the N-terminus of both proteins. The most striking difference is the presence of a positively-charged looping tail (dark blue) at the C-terminal end of GFM1. Structures were computed by MODBASE (Pieper et al., 2004).



Figure 1.4 The Life Cycle of *Drosophila*. The reproductive cycle of the fly takes about 12 days at 25C. Eggs hatch into the first of three larval instages after about one day. During the next 48 hours, two more molts occur to produce the second and third instar stages. After two days, the third instar larvae wander out of the food, form pupae, and undergo metamorphosis. About one week later, the adult fly ecloses from the pupa case. Adult flies can begin the reproductive cycle anew within 8-12 hours of eclosion.

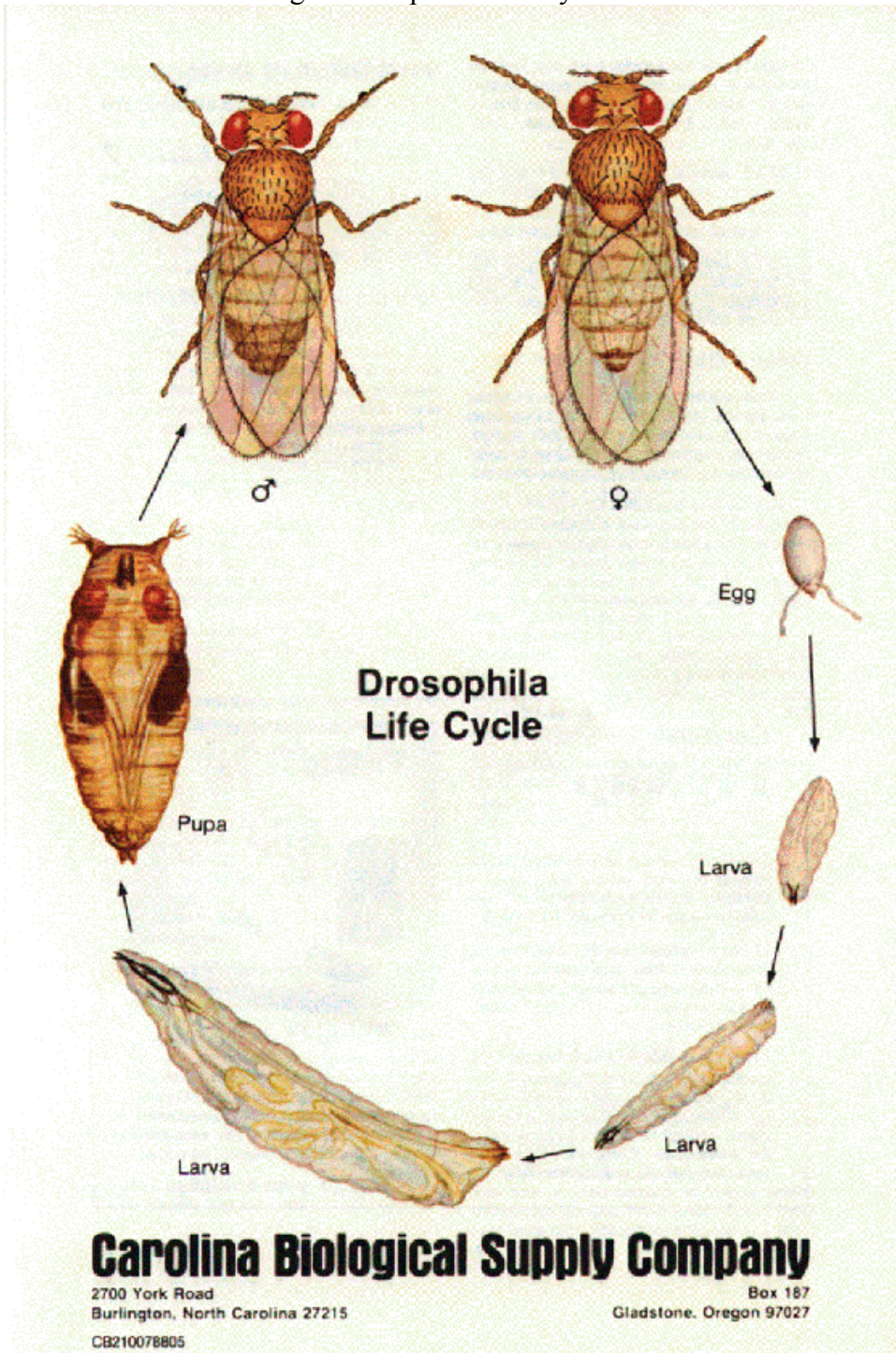
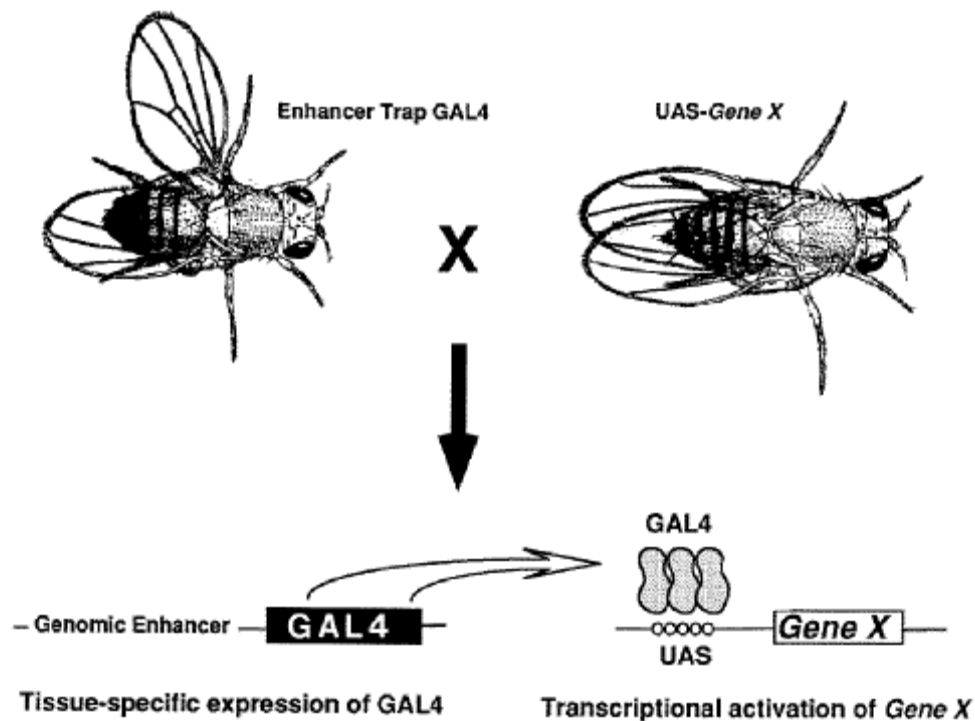


Figure 1.5 The *Drosophila* UAS-GAL4 System. Brand and Perrimon developed the UAS-GAL4 system to allow control of tissue- and temporal expression of transgenic constructs (Brand & Perrimon, 1993). In this system, two different parental strains of flies are crossed together. The first, called a “driver” line, contains an enhancer trap with the expression of the yeast GAL4 transcription factor controlled by a nearby genetic enhancer. The second line contains a target construct with a transgene of interest placed downstream of the GAL4 binding sites known as *Upstream Activating Sequences* (UAS). In progeny with both the GAL4 driver and the UAS-target gene construct, GAL4 will be expressed in a tissue- and temporal-specific manner, depending on the enhancer used, and this will in turn drive specific expression of the target transgene. Figure adapted from (Brand & Perrimon, 1993).



CHAPTER 2

MATERIALS AND METHODS

Fly Strains

Except where otherwise noted, flies were maintained on standard fly medium (Bloomington *Drosophila* stock center recipe) at 25 degrees Celsius. Unless otherwise indicated, fly stocks were obtained from the Bloomington Drosophila Stock Center.

ico point mutant lines: The mutant *II302 (ico^{II032})* flies were generated in an EMS mutagenesis screen of the second chromosome (Nüsslein-Volhard et al., 1984). This mutagen randomly creates point mutation lesions (Huang & Baker, 1976). The *ico^{BA18}*, *ico^{GA1}*, and *ico^{GA25}* alleles were also created by EMS mutagenesis (Tiong & Nash, 1990).

Generation of ico deletion mutants: The deletion alleles *ico^{Del EY1}* and *ico^{Del EY2}* were generated by mobilization of the P-element insertion *EY05983* (Bloomington stock #17583). To do this, a source of transposase, *Delta 2,3* (Robertson et al., 1988), on a balanced, *Stubble (Sb)*-marked third chromosome was crossed to the *w⁻/w⁻* ; *EY05983/EY05983* stock. Mosaic progeny were crossed out to the second chromosome balanced stock *w⁻/w⁻* ; *Gla/Cy*. Progeny with white eyes (indicating excision of the P-element) that lacked the *Sb* marker were then individually crossed to the *w⁻/w⁻* ; *Df(2L)Exel6017/Cy* stock (Bloomington stock number 7503) in which the *Df(2L)Exel6017* deficiency removes *ico*. This cross acted as a complementation test:

crosses in which all the progeny contain a *Gla* or *Cy* balancer indicate a lack of complementation between the mutagenized chromosome and the deficiency. Of the four hundred individual crosses set up, two yielded lethal mutations that did not complement *Df(2L)Exel6017*. *Cy*-balanced stocks were generated for each of these two mutations, *ico*^{*Del EY1*} and *ico*^{*Del EY2*}. Complementation crosses between the *ico*^{*H032*}/*Cy* stock and each of these new mutant stocks indicated that both deletion mutations affect *ico*. PCR performed on genomic DNA from the *ico*^{*Del EY1*} and *ico*^{*Del EY2*} stocks using the primers 5' TTTCCCTATTG-CTCTCGCACG and 3'-ACAGAGTTCTATCCCAGATGAG indicated the presence of deletions in *CG4567*. These deletions were confirmed by sequencing.

Isogenization of fly lines: The *ico*^{*H032*}/*Cy* and *ico*^{*Del EY2*}/*Cy* stocks were isogenized with *yw* flies as follows. Females from each mutant stock were crossed to the same *yw* male. Non-*Cy* female progeny were collected, and this was repeated for three generations. The *ico* mutant lines were re-balanced with a *Gla* marked chromosome, and complementation tests with the original lines were performed to check these new stocks.

UAS-GAL4 drivers: UAS-GAL4 drivers, used for transgene expression as described in the text, were *daughterless-GAL4*, *armadillo-daughterless-GAL4*, *A9-GAL4*, and *patched-GAL4*.

RNAi transgenic flies: The transgenic fly stock #V34874 containing the *UAS-icoRNAi* expression construct was obtained from the Vienna Drosophila RNAi Stock

Center. Expression of this construct was driven with the *daughterless-GAL4* driver as described in the text.

Mapping of *ico*

Complementation testing was performed as follows. The *ico*^{H032}/Cy stock was crossed out to each of three Cy-balanced Exelixis lines: *Df(2L)Exel8019*, *Df(2L)Exel6017*, and *Df(2L)Exel7031* (Bloomington stock numbers 7803, 7503, and 7804, respectively). The progeny from each cross were evaluated for the presence of non-Cy animals, which were indicative of complementation. The *Df(2L)Exel6017* line did not complement *ico*^{H032}, demonstrating that the *ico* locus falls within the *Df(2L)Exel6017* deficiency but outside the other two.

P-element mutagenesis was used, as described above, to create deletions in the five candidate genes. In addition to the P-element *EY09583*, which was used as described above to create deletions in *CG4567 (ico)*, three other P-elements in the region (see FIG 3.1) were also excised. Of these, the PNdae line was obtained from the Bloomington stock center (stock #14423), the SH0319 line was obtained from the Szged Stock Center in Hungary, and the Ndae1K0316 line was obtained from the authors of the paper describing it (Romero et al., 2000; Sciortino, Shrode, Fletcher, Harte, & Romero, 2001). Although four hundred complementation tests were performed for each of these three lines, only excision of the P-element *14423* stock generated additional deletions that were allelic for *ico*. PCR using nested primers indicated that both of these deletions were very large and thus not useful for mapping purposes.

Sequencing of *ico* missense alleles: Each of the four stocks with *ico* point mutations balanced over *Cy* were allowed to lay eggs on apple juice agar plates overnight. Embryos were aged for 30-42 hours, by which time viable offspring had hatched and developed into larvae. Non-viable, unhatched embryos homozygous for an *ico* point mutation were then collected with forceps. For each of the four EMS mutant strains, approximately 35-50 embryos were collected, and genomic DNA was prepared and used for PCR. The amplicons of the *ico* region were gel isolated, phenol:chloroform extracted, precipitated with ethanol, resuspended in water and sent out to Davis Sequencing (Davis, CA).

Bioinformatics

The sequence alignment (FIG 3.3) of ICO and human GFM1 was performed using the ClustalW function of the MacVector bioinformatics program.

Percentage identity between ICO and related orthologues (Table 3.1) was performed by BLAST.

Ribbon structures of GFM1 and GFM2 (FIG 1.2) were computed by MODBASE (Pieper et al., 2004).

Molecular Biology

The transgenic construct for wild-type *ico* was created from a cDNA extracted by PCR from a *Drosophila* embryonic cDNA library (Brown & Kafatos, 1988) using the primers 5'ACAGAGTTCTATCCCAGATGAG and 5' GCGCCTCGAGCTAGTTCTTCTTTTCTTCTTGTC and cloned into the BglII and XhoI sites of *pUAST*. The C-terminal deletion forms for wild-type and *ico*^{H032} were generated from the original constructs using the C-terminal PCR primer

GGCCTAGGCCAATCCTTGCGACTCC. The human *GFM1* construct was generated using a clone ordered from ATCC (#10436473), which was comprised of the full-length *GFM1* cDNA inserted into the pCMV-SPORT6 vector. The human *GFM1* cDNA was PCR amplified from this clone using the primers 5'GTGCGGTACCGGCAGCTGAACCCAC and 5'GCCTCTAGAGTCAGTCAACTCACAGTAAG AND the fragment was cloned into the Asp718 and XbaI sites of *pUAST*. To create the *CG31159* (*Drosophila GFM2*) transgenic constructs, the *CG31159* cDNA was amplified from an embryonic library (Brown & Kafatos, 1988) using the primers 5'TTTAGATCTGAAAATGCTGAAAT-ATGCATGGC and 5'GGCCGCTAGCTATTCAAGGCCCTGTGCTCTG and cloned into the BglII and XbaI sites of *pUAST*. The mutant *ICO-G538E*, *hGFM1-N174S*, and *hGFM1-S321P* transgenic constructs were created by performing site-directed mutagenesis on the respective wild-type constructs using the QuikChange method (Stratagene, La Jolla, CA). Transgenic constructs were sequenced by Retrogen and injected to generate transgenic animals by Genetic Services. Expression of transgenic constructs was performed using the *UAS-GAL4* system using the driver lines described in the text.

Genetics

Enhancer and suppressor screens for interactions with TGF-beta signaling:

Two genetic screens were used to look for novel components of the TGF-beta signaling pathway (and pulled out the *ico*^{H032} mutation). The first, a genetic enhancer screen was performed as described in (Raftery, Twombly, Wharton, & Gelbart, 1995). Progeny were scored to identify maternal and zygotic interactions. The second screen was a

genetic suppressor screen performed as described in (Hoodless et al., 1996). Both of these assays were repeated for the *ico*^{Del EY1} and *ico*^{Del EY2} *ico* alleles, with no interaction found.

Clonal analysis of ico alleles in the eye: In order to generate eye clones homozygous for *ico* mutations, crosses were performed as follows for each of the six *ico* mutant alleles: *white, eyeless-Flipase/ Y; white*⁺, *cell-lethal(2L) FRT(2L)/CyO* males were crossed to *white/ white; ico, FRT(2L)/CyO* females. Since the Flipase is located on the X-chromosome, recombination only occurs in the eyes of female progeny that was examined for the presence of white, non-colored cells derived from recombinant clones of homozygous *ico* mutants.

Behavioral Assays

Hyperthermia: Flies were knocked out with carbon dioxide and sorted into groups of ten at least twenty-four hours before the experiments to avoid possible artifacts from the anesthesia. These groups were placed into standard food vials at 25C, then were transferred to empty vials immediately before the experiment. Each vial was placed in the hyperthermia chamber at 41.5C for 650 seconds, and the time to failure was recorded for each fly using the a program written for our lab called MAMER program. Failure was defined as loss of locomotor activity for more than 10 seconds. After 650 seconds, the vials were removed and placed at room temperature (about 25C). Vials were gently tapped once per second, and recovery time for each fly was recorded. Recovery was defined as regaining locomotor activity and moving away from the tapping stimulus at the bottom of the vial. Data was analyzed (one-way ANOVA) and graphs generated using Sigma Stat and SigmaPlot software. For these experiments,

each vial of ten flies counted as an N of one. A minimum of eight trials for each treatment was performed.

Anoxia: For these experiments, flies were anesthetized and sorted into groups of ten as in the hyperthermia experiments. The experimental vials (each fitted with a porous foam lid) were then placed into an anoxia chamber which was filled with inert argon gas at a pressure of 110 mm Hg. After twenty minutes, the vials were taken out of the chamber, the lids were removed, and the vials were rolled to remove the argon and restore atmospheric gasses. The lids were then replaced, the vials were tapped once per second, and recovery time was recorded as in the hyperthermia experiments. Analysis was performed (one-way ANOVA) and graphs generated using the Sigma Stat and SigmaPlot software, with each vial of ten flies counting as an N of one. A minimum of eight trials was performed for each treatment.

Accession Numbers: *CG4567 (ico)* mRNA- NM135261, human *GFMI* mRNA – NM 024996

CHAPTER 3

IDENTIFICATION AND CLONING OF *ICONOCLAST*

INTRODUCTION

II032 is an EMS-induced mutation generated more than twenty years ago in the Nüsslein-Volhard and Wieschaus mutagenesis screen (Nüsslein-Volhard et al., 1984). It is recessive lethal, with homozygotes exhibiting head-involution defects and dying during late embryogenesis. *II032*'s approximate location was originally mapped to the 28C region of the left arm of chromosome two, but due to technological constraints the gene affected was not identified. This mutation was not characterized further and consequently was not given a name.

More recently, our lab found that *II032* gave a positive result in screens for genes with potential interactions with the TGF-beta signaling pathway (Raftery et al., 1995), a cellular pathway that plays important roles in embryonic development (Hoodless et al., 1996), the regulation of cell proliferation and apoptosis (Cain & Freathy, 2001), as well as the development and progression of cancer in humans, reviewed in (Rooke & Crosier, 2001). Because it was identified using a screen to find signaling components that are not part of the canonical TGF-B pathway, we decided to name this locus *iconoclast* (*ico*). Although the genetic interaction of was later determined to be due to gain-of-function effects of the *II032* mutation and does not necessarily represent a normal function of the gene (as described later in this

manuscript), it became clear that *ico* is crucial for normal development and viability.

Discovering the identity of this vital gene would be the essential first step in elucidating the important roles played by *ico*.

RESULTS

Mapping of *iconoclast*

In order to acquire additional alleles of *ico*, complementation tests were performed on several strains of flies created in a EMS mutagenesis screen of the 27-28 region of chromosome two (Tiong & Nash, 1990). Briefly, if a fly carrying a recessive lethal mutation in a certain gene is crossed to a fly carrying either a balanced mutation in the same gene or a chromosome carrying a deficiency that removes the gene, progeny that receive both mutations will die, and the fly strains do not complement each other. Complementation tests between these lines and *ico*^{H032} identified three additional alleles of *iconoclast*: *ico*^{BA18}, *ico*^{GA1}, and *ico*^{GA25}. Unfortunately, the gene affected by these mutations had not been identified.

To facilitate more precise mapping of *ico*'s location, several strains of flies carrying classical deficiencies in the 27-28 area were obtained. These deficiencies often remove large portions of the chromosome and can be used to perform complementation tests to determine the approximate location of a recessive lethal mutation. Using these deficiencies, the search was narrowed down to region in 27E. Unfortunately, the endpoints of classical deficiencies are not precisely mapped, reducing the precision of this method.

Fortunately, at this time, the Excelix Corporation made available to the fly community several hundred deficiencies that it had generated. Unlike classical

deficiencies, which were often created by X-ray or P-element mutagenesis, the precise endpoints of the Exelixis deficiencies (and thus the genes deleted by these deficiencies) can be determined. Using these deficiencies, the search was narrowed to a region that contained five predicted genes. (FIG 3.1).

Ideally, complementation testing with mutants in each of these five genes could reveal the identity of *ico*. However, a search of Flybase as well as the Bloomington and Szged stock center websites revealed that no lethal mutant stocks were available for any of these five candidate genes. To create new deletion mutations in this area, four P-elements (transposons) in this region (FIG 3.1, blue arrows) were used to induce transposon-mediated mutagenesis in these genes. These P-elements are hobbled and lack the functional transposase enzyme required to mobilize them. When the transposase source Delta-2,3 is crossed into a fly strain containing one of these P-elements, the transposon can be “jumped out” and excised. A small percentage of the time, imprecise excision of a P-element may result in the loss of DNA flanking the insertion site (Preston, Sved, & Engels, 1996). The frequency of mutagenesis and the average size of the deletions created can vary, depending on the location of the P-element.

Each of the four strains containing one of the four transposons of interest was crossed with flies containing the Delta-2,3 transposase source. The resulting mosaic progeny were each separately crossed to the double-balanced stock *Gla/CyO*. Progeny from this second set of crosses were scored for eye color, as loss of the red eye color indicates that the transposon has been excised. For each of the four transposon lines, at least 400 white-eyed progeny were collected and each were crossed separately to

7503/CyO, a stock containing one copy of the second chromosome deficiency 7503 (which removes *ico*) and a balanced second chromosome that harbors a marker for curly wings. These complementation crosses allowed identification of lethal transposon-mediated deletions in the region, as these deletions would be unable to survive in combination with the 7503 deficiency. Such crosses are easily scored: for a positive “hit”, all the adult progeny from the cross will have at least one balancer chromosome.

Four positive hits for lethal mutations within the 7503 region were identified – two from excision of the *EY05983* P-element and two from the excision of *I4423*. For each of these positive hits, balanced white-eyed sibs were crossed to create balanced stocks of these deletion mutants. All four of these novel mutations failed to complement *ico*^{*H032*}, demonstrating that they each represent mutations in *ico*. Interestingly, unlike the missense alleles, these new deletion alleles of *ico* did not interact when tested with the genetic enhancer and suppressor screens described above.

PCR was then performed using sets of primers spaced throughout the region to identify the location of each deletion. Results indicated that both the deletions derived from *I4423* are very large. However, the *ico*^{*Del EY1*} and *ico*^{*Del EY2*} deletions removed smaller regions about 1.9 and 3.7 kb in length, respectively, from the predicted gene *CG4567*, suggesting that this gene is the *iconoclast* locus.

Confirmation that *ico* is CG4567

To further investigate whether *ico* is *CG4567*, the four EMS-induced alleles of *ico* (*ico*^{*BA18*}, *ico*^{*GA1*}, and *ico*^{*GA25*} and *ico*^{*H032*}) were sequenced to look for missense or nonsense mutations. To do this, for each strain, DNA was prepared from a small number of embryos homozygous for the mutation. When laid on apple juice plates,

these embryos could be distinguished from unfertilized eggs and heterozygous embryos because they begin development but fail to hatch after 24 hours, dying and turning brown before 48 hours post egg-laying. The gene *CG4567* was PCR amplified from this DNA (using a proof-reading polymerase to minimize errors), and the amplicons for each strain were sent out for sequencing. Sequencing results revealed missense mutations in all four alleles (FIG 3.2) compared to the wild-type sequence provided by Flybase and NCBI (Accession #NP_609105). To confirm that these are true mutations and not the result of either errors that occurred during amplification or sequencing or an error in the annotated sequence, fresh DNA was prepared from heterozygous animals. Performing PCR with this DNA should result in the amplification of approximately equal amounts of both the wild-type and *ico* allele from each strain. Thus, when examining the histograms of each set of sequencing results, it was possible to verify the accuracy of the annotated sequence as well as confirm the presence of the mutations identified in the first set of sequencing reactions (which easily stood out as pairs of overlapping peaks on the histogram). These experiments confirmed that significant mutations are found in the *CG4567* coding region in each of the four EMS-induced *ico* mutant strains, su

In order to confirm this hypothesis and prove that *iconoclast* is *CG4567*, a transgenic construct was created to express wild-type *CG4567 in vivo*. If *CG4567* is *iconoclast*, expression of this protein should rescue lethality in *ico* deletion mutants. To test this, the *CG4567* cDNA was amplified from a *Drosophila* embryonic cDNA library (Brown & Kafatos, 1988) and cloned into *pUAST*, a vector that allows for transgene expression *in vivo* using the *UAS-GAL4* system (Brand & Perrimon, 1993). The

construct was sent out for microinjection, and stable transgenic fly strains were established.

As mentioned previously, the *Drosophila* UAS-GAL4 expression system allows for the temporal and spatial control of expression of transgenic constructs.

When the *UAS-CG4567* transgene is ubiquitously expressed under the combined control of the *armadillo-GAL4* (*arm-GAL4*) and *daughterless-GAL4* (*da-GAL4*) drivers, it rescues the lethality of homozygous and transheterozygous (a combination of both alleles) *ico* deletion mutations. (These drivers were chosen because together, they strongly drive expression in a ubiquitous manner, beginning during early embryogenesis. These results clearly demonstrate that *iconoclast* is *CG4567*).

Sequence and Functional Conservation of ICO and Human GFM1

So, what type of protein does *iconoclast* encode? Sequence comparison by Blastx (Table 3.1) suggests that *ico* is the *Drosophila* orthologue of *mitochondrial translation elongation factor G1* (*GFM1*), which is highly conserved in eukaryotes. The ICO protein is highly homologous (73.7% identical) to the human GFM1 orthologue (FIG 3.3). In order to ascertain whether the functions of the proteins encoded by these two genes are also conserved, an experiment was performed to determine whether expression of human GFM1 could compensate for a loss of *ico* and rescue the lethality of *ico* mutations.

To do this, the human *GFM1* cDNA was obtained from ATCC (#10436473) and was cloned into the *pUAST* vector to create the transgene *UAS-hGFM1* which could be expressed in flies using the *UAS-GAL4* system. The construct was sent out for microinjection to create stable lines of transgenic flies. Ubiquitous expression of *UAS-*

hGFM1 under control of the *da-GAL4* driver was able to rescue the lethality of *ico* deletion mutants (*ico*^{Del EY2} / *ico*^{Del EY2} or *ico*^{Del EY2} / *ico*^{Del EY1}), producing 91.7% of the expected number of rescued animals (67/73). These results reveal that the human GFM1 protein is similar enough to assume the function of fly ICO, demonstrating that both the sequence and function of these proteins is conserved.

Investigation of Conservation of Function between ICO with CG31159, The Fly GFM2 Orthologue

It is possible that the lethality caused by deletion mutations in *ico* is due to consequences of the reduction in the amount of mitochondrial translation elongation factor proteins which are necessary for mitochondrial biosynthesis. If this is the case, then it may be possible to rescue this defect by overexpressing the *GFM2* orthologue *CG31159*, thus increasing the amount of mitochondrial translation elongation factor proteins. To test this hypothesis, a *UAS-CG31159* construct was created and expressed ubiquitously with a combination of the *daughterless*- and *armadillo-GAL4* drivers. Expression of *CG31159* failed to rescue *ico* deletion mutants, indicating that restoring the amount of translation elongation factor is not sufficient to redress the effects of loss-of-function *ico* mutations. This is consistent with the previously mentioned studies in which human GFM2 could not rescue the phenotype of mutations in GFM1 in human fibroblasts. These results suggested that perhaps ICO (and other GFM1 orthologues) may have a function in addition to its role as a mitochondrial translation elongation factor. Alternatively, the subsequent work by Tsuboi et al. demonstrating that at least one isoform of GFM2 protein acts as a recycling factor and has little elongation activity,

at least *in vitro*, is also consistent with these results and suggests that overexpression of GFM2 proteins might not confer significant elongation activity.

Deletion of the C-terminal Tail of ICO and Rescue of *ico* Mutations

Perhaps the most striking difference between the mitochondrial translation elongation factor G1 and G2 proteins is the presence of a conserved positively-charged tail at the C-terminus of the GFM1 proteins and their orthologues. As shown above, *CG31159*, which (as a GFM2 orthologue) lacks this tail, does not functionally rescue mutations in *ico*. In order to determine if the C-terminal tail is necessary to rescue the lethality of *ico* mutations, a transgenic construct in which an introduced stop codon results in a truncated the ICO protein, removing just the tail, was created. Ubiquitous expression of this tailless ICO was sufficient to rescue 92.4% of *ico* deletion mutant progeny (61/66 animals). This demonstrates that while the C-terminal tail of ICO may have a function, it is not necessary to rescue viability.

DISCUSSION

It was somewhat surprising to find mutations in a mitochondrial translation elongation factor in two separate screens for novel TGF-beta signaling components. While point mutations interacted with the screens, deletion mutations did not, suggesting that loss-of-function consequences were not the reason for the interaction of missense alleles. Because these missense alleles are from three different genetic backgrounds (as well as the fact that other mutant lines from the same *GA* and *BA* backgrounds did not interact with the screens), this interaction is likely not due to some other mutation in the background of these animals. It is possible that the missense alleles have some additional antimorphic consequences along with loss-of-function

effects, and that these novel effects cause the observed interactions with screens for TGF-beta components.

The hypothesis that missense mutations in *ico* produce additional effects is supported by a comparison of the phenotypes of the two different types of *ico* alleles. While mutants carrying two missense alleles of *ico* die during late embryogenesis, animals harboring two deletion mutations survive much later, until the second or third larval instar stage. This disparity in phenotype suggests that in addition to loss-of-function consequences, *ico* missense mutations result in proteins with toxic effects on the animal. The effects of these proteins, as well as their potential interaction with the TGF-beta screens, will be further addressed later in this manuscript.

These experiments have identified the first mutations in the *Drosophila mitochondrial elongation factor G1* gene, which we have named *iconoclast*. Rescue with human GFM1 demonstrates that not only the sequence but also the function of these two proteins is conserved. In contrast, expression of the fly *GFM2* orthologue *CG31159* is unable to rescue *ico* mutations, suggesting that ICO may have a role in addition to its function as a mitochondrial translation elongation factor. Comparison of phenotypes between missense and deletion mutants suggests that in combination with possible loss-of-function effects, mutant ICO proteins may also have additional, toxic effects.

Figure 3.1 Candidate Genes and P-element Transposons. The location of *ico* was narrowed down to a region in 27E containing five candidate genes: *CG4502*, *CG13784*, *CG4567*, *CG31906*, and *Ndae1*. Four P-elements (blue arrows) in this area were obtained: from left to right, *SH0319*, *EY09583*, *Ndae1-k0316*, and *PNdae (14423)*. Each of these transposons was used for P-element-mediated mutagenesis. When a P-element is mobilized, a small percentage of the time, it removes portions of the DNA flanking the excision site, creating deletion mutations. Two lethal deletion mutations that were allelic for *ico* were obtained from excision of *EY09583* and two much larger allelic deletions were created with *14423*.

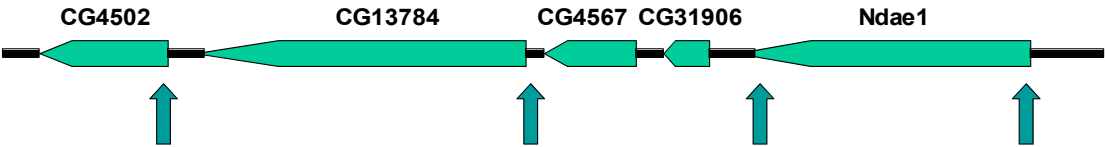
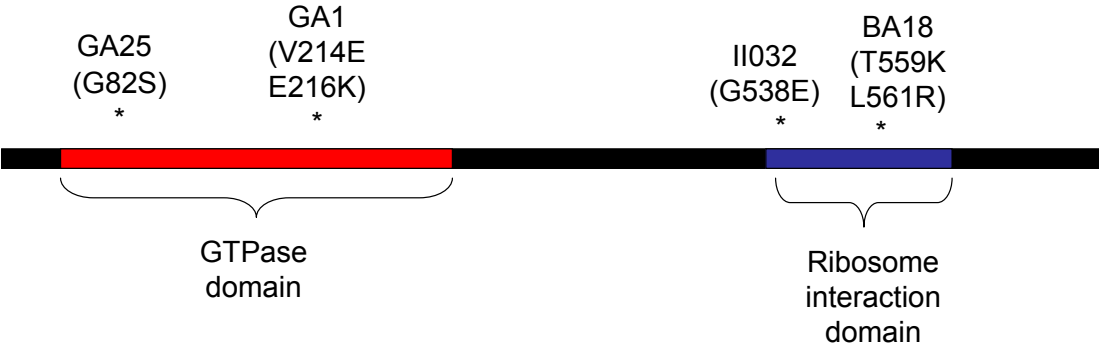


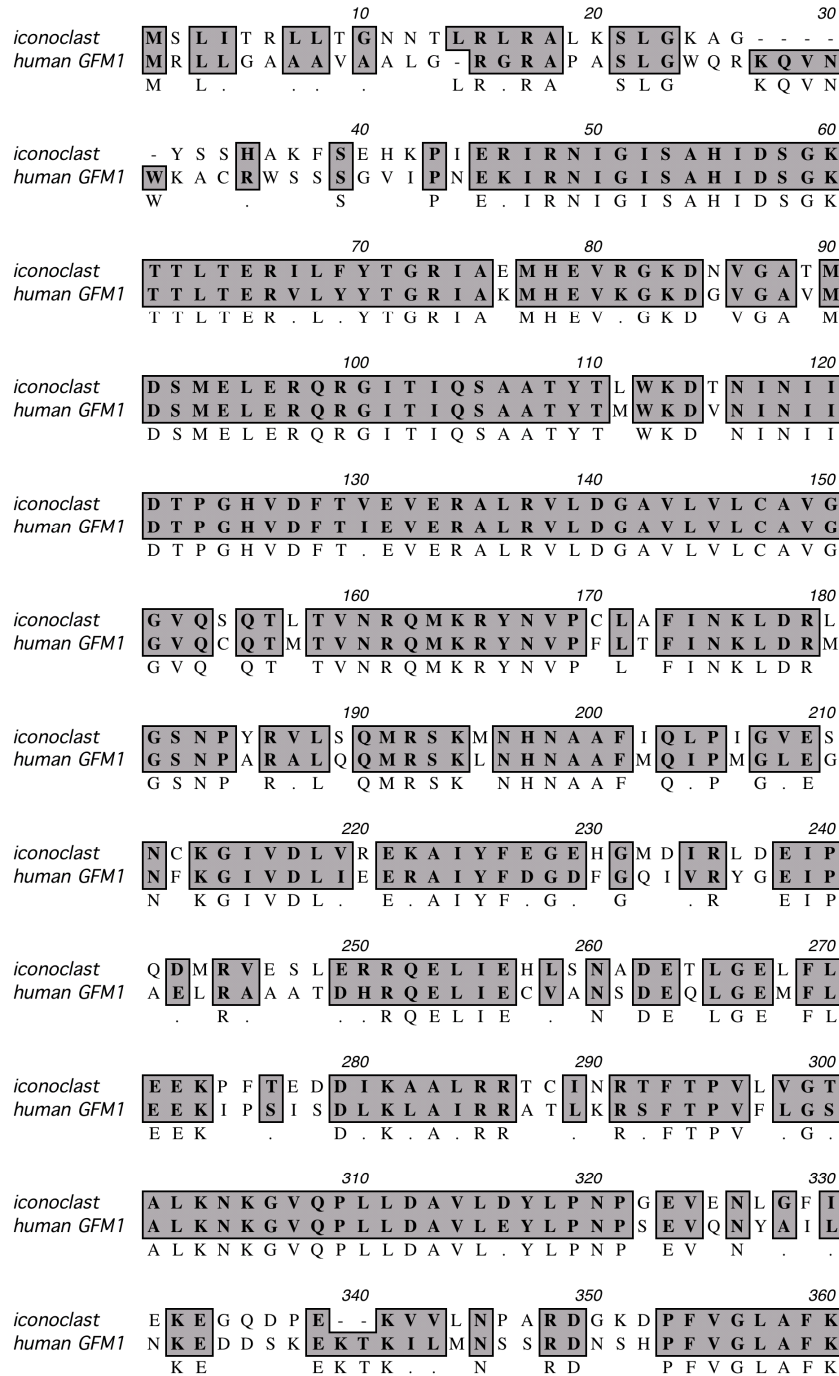
Figure 3.2 Alleles of *iconoclast*. Two point mutation alleles, *ico*^{GA25} and *ico*^{GAI}, affect the GTPase domain of ICO. The other two, *ico*^{II032} and *ico*^{BA18}, affect a domain that is known to associate with the ribosome during translation elongation. The *ico*^{Del EY1} and *ico*^{Del EY2} deletion mutations remove all but the GTPase domain of the protein.



<i>ico</i> allele	<i>ico</i> ^{GA25}	<i>ico</i> ^{GAI}	<i>ico</i> ^{II032}	<i>ico</i> ^{BA18}	<i>ico</i> ^{Del EY1}	<i>ico</i> ^{Del EY2}
Mutation	G82S	V214E; E216K	G538E	T559K; L561R	1888 bp deletion; stop after 6 amino acids past P314	3663 bp deletion; stop after 19 amino acids past C367

Figure 3.3 Sequence Alignment of ICO and Human GFM1. ICO and GFM1 are well-conserved, and as with other GFM1 orthologues, both proteins have a positively-charged C-terminal tail.

Formatted Alignments



iconoclast 370 380 390
 LEAGRFGLTYLR C YQG V LRKGD N IFN A RT
human GFM1 LEVGRFGQLTYVR S YQGE LKKGD T IYNT RT
 LE . GRFGQLTY . R YQG L . KGD I . N RT

iconoclast 400 410 420
 N KKVRI A RLVR L H S N Q MEDV N EVYAGDI F A
human GFM1 R KKVRL Q RLAR M H A D M MEDV E EVYAGDI C A
 K K V R . R L . R H M E D V E V Y A G D I A

iconoclast 430 440 450
 LFGVDCASGDTFT T N P K N N LSMESI F VPEP
human GFM1 LFGIDCASGDTFT D K A N S G LSMESI H VPDP
 L F G . D C A S G D T F T L S M E S I V P . P

iconoclast 460 470 480
 VVSMAI KPN N T K D R D N FSKAIARFTKEDPT
human GFM1 VVISI AM KPS N K N D L EK FSKGIGRFTREDPT
 V . S A K P N D . F S K . I . R F T . E D P T

iconoclast 490 500 510
 FHF FFD N D V KETLVSGMGE L H L E I Y A Q R M E
human GFM1 FKV YFD T E N KETVISGMGE L H L E I Y A Q R L E
 F . . F D . K E T . . S G M G E L H L E I Y A Q R E

iconoclast 520 530 540
 REYGCP V T L GKPKVAFRET L V GP C E F D Y L H
human GFM1 REYGCP C I T GKPKVAFRET I T A P V P F D F T H
 R E Y G C P G K P K V A F R E T . . P F D . H

iconoclast 550 560 570
 KKQSGG S GQYARIIGV M EPL P P N Q N T L L E F
human GFM1 KKQSGG A GQYGKVIGV L EPL D P E D Y T K L E F
 K K Q S G G G Q Y . . . I G V E P L P T L E F

iconoclast 580 590 600
 V DET V GTNVPKQFVP GVE KGY R E M A E K G M L
human GFM1 S DET F GSNIPKQFVPAVE KGF L D A C E K G P L
 D E T G . N . P K Q F V P . V E K G . E K G L

iconoclast 610 620 630
 SGHKLSGIRF R LQDGGHH I VDS S EL A F M L A
human GFM1 SGHKLSGLRF V LQDGAHH M VDS N E I S F I R A
 S G H K L S G . R F L Q D G . H H V D S E . F I R A

iconoclast 640 650 660
 A H GAIK E V F Q NGS W Q ILEPIMLV E V T A P E E
human GFM1 G E GALK Q A L A N A T L C ILEPIMAVE V A P N E
 . G A . K . N . . I L E P I M . V E V A P E

iconoclast 670 680 690
 FQG A V M G H L S KRHGIITG T EGT E G WFTVYA
human GFM1 FQG Q V I A G I N RRHGVITG Q DGV E D YFTLYA
 F Q G V . . . R H G . I T G . G E . F T . Y A

iconoclast 700 710 720
 EVPLNDMF GY A G ELRS S T Q GKGEFTMEYS R
human GFM1 DVP LNDMF GY S T ELRS C T E GKGEY TMEYS R
 . V P L N D M F G Y E L R S T G K G E . T M E Y S R

iconoclast 730 740 750
 YS PCLP D V QD Q IV R Q Y Q E S Q GL A Q P D K K K
human GFM1 YQ PCLP S T QE D V I N K Y L E A T G Q L P V K K G K A
 Y P C L P Q . . Y E G . K K K

iconoclast 760 770 780
 K N
human GFM1 K N
 K N

Table 3.1. Comparison of Identity of Protein Sequences of ICO and GFM1 Orthologues in Other Species. GFM1 proteins are highly conserved in eukaryotes. Strikingly, ICO shares more than 70% percent identity with orthologues in the mouse, frog, zebrafish, and human.

Reference Protein		Species	Id(%)	Len(aa)
NP_609105.1	CG4567	<i>D. melanogaster</i>	100.0	744
NP_613057.2	G elongation factor, mitochondrial 1	<i>M. musculus</i>	74.3	708
NP_001093367.1	hypothetical protein LOC100101315	<i>X. laevis</i>	74.3	708
NP_079272.4	G elongation factor, mitochondrial 1	<i>H. sapiens</i>	73.7	709
NP_001073463.1	G elongation factor, mitochondrial 1	<i>D. rerio</i>	73.3	708
NP_496787.1	hypothetical protein F29C12.4	<i>C. elegans</i>	67.8	709
NP_013170.1	Mitochondrial elongation factor involved in translational elongation; Mef1p	<i>S. cerevisiae</i>	61.6	690
NP_175135.1	mitochondrial elongation factor, putative	<i>A. thaliana</i>	61.4	709
XP_965342.2	elongation factor G 1, mitochondrial precursor	<i>N. crassa</i>	59.4	699
XP_001701845.1	chloroplast elongation factor G	<i>C. reinhardtii</i>	48.6	685

CHAPTER 4

DEVELOPMENTAL PHENOTYPES OF *ICO* MUTANTS

INTRODUCTION

In this chapter, the developmental phenotypes of *ico* missense and deletion mutants are investigated. In addition, the effects of *ico* knockout on the development of adult tissues and the consequences of *ico* knockdown in whole adult animals are examined.

Recessive Lethality of *ico* Mutations

As mentioned in chapter one, flies heterozygous for any of the four *ico* missense alleles (*ico*^{*II032*}, *ico*^{*BA18*}, *ico*^{*GAI*}, and *ico*^{*GA25*}) die during embryogenesis. In addition, transheterozygous combinations of *ico* alleles are also embryonic lethal. Very rarely, (about one out of every 200 animals), *ico*^{*GA25*}/*ico*^{*GA25*} mutant animals survive embryogenesis and hatch as small first instar larvae. These few larvae exhibit greatly reduced movements and die within hours of hatching from the egg.

In contrast, flies homozygous or transheterozygous for the *ico* deletion alleles *ico*^{*Del EY1*} and *ico*^{*Del EY2*} survive much longer, making it to the second or early third larval instar stage before dying. These mutant larvae are thinner than wild-type larvae, possibly because of either metabolic disruption or reduced movements resulting in reduced feeding behavior. Heterozygous animals with one copy of a missense allele

and one copy of a deletion allele have an intermediate phenotype; these animals die as late first instar larvae.

It is striking that *ico* deletion mutants live much longer than missense mutants. This indicates that the production of mutant ICO protein is worse than not producing functional ICO at all, consistent with the hypothesis that mutant ICO proteins may have additional harmful gain-of-function or antimorphic effects.

Phenotypes of Heterozygous *ico* Mutants

In contrast to the lethality observed in homozygous or transheterozygous *ico* mutants, flies harboring one mutant copy of *ico* (missense or deletion allele) and one wild-type copy are viable and fertile. For each of the six *ico* alleles, stocks balanced over *CyO* or *Gla* second chromosomes are easily maintained. These stocks do not appear sickly or lacking in fecundity. For the most part, no gross physical abnormalities are observed in these flies, except that flies heterozygous for *ico* missense mutations develop brittle wings by 10 days post-eclosion. This phenomenon is most noticeable when picking up the flies by the wing with a pair of forceps. In contrast, brittle wings are usually characteristic of older flies. Flies heterozygous for *ico* deletion alleles do not show this change in their wings.

RNAi Loss-of-Function Phenotypes

In addition to using the *UAS-GAL4* system to control expression of transgenes, the *GAL80* system may be used as described in the introduction to turn this expression on or off as a function of temperature reviewed in (Duffy, 2002). In this way, transgenes may be selectively expressed (under control of the same GAL4 driver) during specific stages of development. Ubiquitous expression with the *da-GAL4* driver

of a transgenic *CG4567 (ico)* RNAi construct (along with *Dicer2*) obtained from the Vienna Stock Center has varying effects, depending on when it is expressed. Expression of *ico* RNAi during embryogenesis or larval development is lethal. However, if the *GAL80* system is used to suppress expression of *ico* RNAi until one week after flies eclose and reach adulthood, no lethal effects are seen. These adult knock-down animals did exhibit a hyperkinetic phenotype: even in the incubator, without additional outside stimulus, the animals moved frenetically around their vials with unusual jerky motions that were reminiscent of that seen in *ico* mutant animals exposed to hyperthermia (see Chapter 6). Of the 30 knockdown adults collected, 22 of them were still alive 26 days after initiation of expression of the RNAi construct, versus 14 out of 30 control flies. Fecundity was also preserved. After 26 days, the animals were used for acute stress experiments (described in Chapter 6).

Effects of *ico* Mutations on Somatic Cells

The above results demonstrate that ICO is essential during development. However, the RNAi experiments suggest that ICO is not crucial in adult animals. It is possible that ICO may play a role during development that is not required in all tissues or adult animals. As a first step to compare the effects *ico* deletion and point mutations have on somatic cells, the developmental fate of homozygous mutant clones in the eye was investigated using the FRT/Flipase system (Stowers & Schwarz, 1999). Since this tissue is non-essential, mutant clones in the eye do not affect viability and development to the adult stage. To perform this experiment, each of the six *ico* mutations were recombined with an FRT-containing transgene close to the centromere on the left arm of chromosome 2 (2L), where *ico* is located. When the yeast recombination enzyme

Flipase is expressed under the control of *eyeless* regulatory sequences in eyes of a heterozygous animal with two FRT sites at the same position on the two sister chromosomes, somatic recombination of the chromosomal arms can occur during mitosis, resulting in daughter cells that contain two wild type and two mutant copies. Clones derived from heterozygous cells that do not recombine are red, while clones homozygous for *ico* mutations are white. The recessive cell-lethal (2L) was used to eliminate homozygous wild-type cells which might otherwise out-compete homozygous mutant *ico* clones and suppress their proliferation.

Our results show that eye clones homozygous for *ico*^{H032} do not survive (FIG 4.1A), and we detect only non-recombined red cells in the eyes of these animals. The size of the eyes is reduced and patterning is disrupted, since only cells that did not recombine survive and proliferate. Compared to *ico*^{H032}, a few small clones of white homozygous *ico*^{GA1} and *ico*^{BA18} cells are present in adult eyes (FIG 4.1B and C, arrow), indicating that the few homozygous mutant cells that do survive may not proliferate well. Among the point mutation alleles, *ico*^{GA25} produces the largest clones with the most white cells (FIG 4.1D); however, the size and patterning of the eye is altered. In contrast, we can find large clones of the homozygous deletions *ico*^{Del EY1} or *ico*^{Del EY2} (FIG 4.1E and F). In these animals, most eyes are normal in shape and only occasionally exhibit small pattern defects, primarily at the periphery. The results of this assay illustrate that point mutations and truncations in ICO have quite distinct effects on cell proliferation and survival. While clones of null mutations survive to adulthood in large numbers, clones of point mutations experience significant levels of cell death. This finding suggests that point mutations are not just loss-function mutations but

encode proteins that are toxic to the cell. Since *ico*^{H032} clones exhibit the highest level and *ico*^{G425} clones the lowest level of mortality, it appears that point mutations differ in their toxicity.

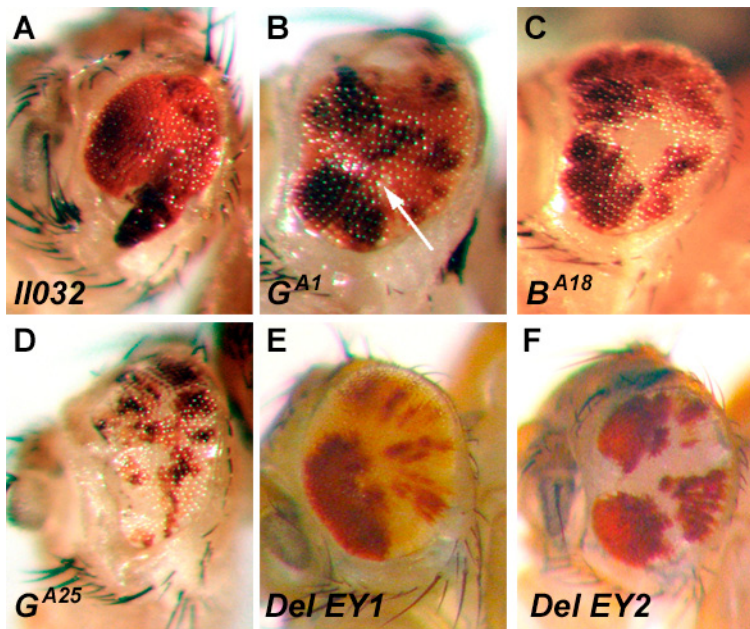
DISCUSSION

It is striking that while ICO is required during development, it does not appear to be as crucial in certain tissues and adult animals. Both eye clones null for *ico* as well as adults expressing *ico* RNAi are viable. It is possible that the second GFM protein in flies, encoded by *CG31159*, is sufficient to promote mitochondrial translation elongation in adult animals. If this is the case, it may be that the processes of development require so much energy that knockdown or knockout of one of the two GFMs is lethal. This hypothesis is contradicted by the fact that ubiquitous overexpression of *CG31159* cannot rescue *ico* mutations, as described in Chapter 3. Further evidence against this hypothesis is offered by the previously mentioned experiments in *C. elegans* indicating that knockdown of the *Gfm1* orthologue in worms is lethal, while knockdown of the worm *Gfm2* is not, suggesting a mere reduction in the amount of mitochondrial translation elongation factors is not sufficient to cause lethality. Alternatively, it is possible that ICO plays a role during development in addition to its function as a translation elongation factor, and that disruption of this additional role is responsible for the lethality of *ico* mutant and knockdown animals.

The results of the eye clone experiment demonstrate that while *ico* is not necessary in at least some somatic cells, missense mutations in *ico* have deleterious effects on proliferation and survival. This suggests that these mutant ICO proteins have toxic, antimorphic effects. This is consistent with the more severe lethal phenotype

seen in missense mutant versus deletion mutants. While the harmful effects of *GFM1* mutations in human patients were assumed to be the result of loss-of-function consequences, these results demonstrate that it is possible for toxic, antimorphic effects of mutations in GFM1 orthologues to also have significant impact.

Figure 4.1 Clonal Analysis of *ico* Mutants in the Eye. Clones of homozygous *ico* alleles were generated with *eyeless*-Flipase in the eyes of females. Pigmented cells are heterozygous for *ico*, while homozygous *ico* clones do not contain eye pigment and are white. In contrast to clones of missense mutations that do not survive to adulthood and lack (A) or exhibit a small numbers of white cells (B-D), clones of truncation mutations develop normally (E and F). While that latter result indicates that ICO is not required during eye development, the former result shows that full-length missense mutant proteins exhibit deleterious effects.



CHAPTER 5

EFFECTS AND SUBCELLULAR LOCALIZATION OF MUTANT ICO PROTEINS

INTRODUCTION

Results presented in the previous chapter demonstrate that *ico* missense alleles produce protein with harmful antimorphic effects. In this chapter, the effects of mutant ICO, as well as the role of the C-terminal tail, are examined. The functionality of mutant human GFM1 proteins is also investigated.

RESULTS

Harmful Effects of ICO^{H032} Expression

In order to further investigate the harmful effects of mutant ICO proteins, expression of mutant ICO in animals with wild-type backgrounds was examined. To accomplish this, a transgenic construct was created. This construct is similar to the *UAS-ico* (*UAS-CG4567*) construct, except that the *ico* gene was altered (by the Strategene Quikchange method) to introduce the G538E (*ico*^{H032}) mutation. The resulting transgene (*UAS-CG4567-G538E*) will express the mutant *ico*^{H032} allele when activated by a GAL4 driver. This mutant allele was chosen because it had the strongest effect in the eye clone assays.

The da-GAL4 driver was used to express two copies of the *ico*^{H032} allele in a ubiquitous pattern throughout development in animals with two wild-type copies of *ico*. (Because position effects of transgene insertion sites can influence expression levels,

two copies of the transgene were recombined onto the same chromosome to ensure strong expression). Expression of *ico*^{*II032*} was lethal, with animals dying as first or second instar larvae. The fact that these animals had two normal copies of *ico* suggests that this lethality is not the result of loss-of-function consequences but rather the toxic effects of the mutant ICO protein. In contrast, expression of two copies of the wild-type ICO construct *UAS-CG4567* did not cause lethality.

Next, the toxic effects of this protein were further examined by expressing the *ico*^{*II032*} allele in the wing, a non-essential organ (FIG 5.1). First, the *ptc-GAL4* driver was used to drive expression of ICO^{*II032*} in the area between longitudinal veins 3 and 4. Expression of the mutant protein disrupts patterning and inhibits formation of the anterior crossvein (FIG 5.1B, compare to normal wing, FIG. 5.1G). A reduction in the number of cells in this area was also seen with expression of ICO^{*II032*}, suggesting that the mutant protein may also inhibit proliferation. (This is consistent with the results observed in the eye clone experiment.) Next, the effects of ICO^{*II032*} expression in the whole wing were observed by driving expression with the *A9-GAL4* driver. Expression of the mutant protein throughout the wing resulted in both patterning defects (conversion of intervein tissue to vein tissue) and alteration of dorsal-ventral proliferation rates (FIG 5.1D). In contrast, expression of wild-type ICO with the same driver did not affect patterning (FIG 5.1C).

Contribution of the C-terminal Tail to Toxic Effects of ICO^{*II032*}

As noted in Chapter 1, although GFM1 orthologues in eukaryotes are very similar to GFM2 proteins (and cytosolic translation elongation factors as well). The most striking difference is the presence of a positively-charged tail at the C-terminal

end of GFM1 orthologues. The conservation of this tail in all GFM1 orthologues from yeast to humans suggests an important role for this domain. To access the role, if any, of this tail on patterning and growth inhibition, two new *UAS* transgene constructs were created in which strategically inserted stop codons result in the production of tailless ICO proteins: one construct to create a tailless ICO^{H032} protein, and the other to create a tailless wild-type ICO protein.

Interestingly, unlike native ICO^{H032} proteins, ubiquitous expression of tailless ICO^{H032} in the wing does not have a negative effect on proliferation or growth (FIG 5.1 F). Expression of wild-type ICO with the tail removed also does not impact development in the wing. These results demonstrate that the C-terminal tail plays a permissive role in the harmful effects exhibited by mutant ICO.

Role of the C-terminal Tail in Localization of Mutant ICO

In order to further investigate the essential role played by the C-terminal tail in the harmful effects of mutant ICO proteins, the effects of this tail on the stability and subcellular location of mutant and wild-type GFP-tagged ICO proteins was examined. A modified *pUAST2* vector was used to allow expression of GFP-tagged ICO and CG31159 proteins with or without the mitochondrial target protein sequence (TP) and with or without the C-terminal tail in *Drosophila* Schneider 2 (S2) tissue culture cells. To express the fusion proteins in S2 cells, the *pUAST2* constructs were co-transfected with an *actin5C-GAL4* driver plasmid.

Four days after transfection, robust expression of all the fusion proteins studied was detected by confocal microscopy, indicating that these proteins are not degraded. GFP is observed in the nucleus and cytoplasm of the cell (FIG 5.2 A). Compared to

GFP alone, localization of GFP-tagged ICO (GFP-CG4567) and ICO^{II032} (GFP-CG4567-G538E) proteins which lack the mitochondrial targeting sequence is predominately nuclear (FIG 5.2 B and C). Deletion of the C-terminal tail from GFP-tagged ICO protein reverts to a diffuse cytosolic and nuclear localization pattern, suggesting that the C-terminal tail may be responsible for enhancing nuclear localization (FIG 5.2 D). A CG31159 fusion protein (GFP-CG31159) that lacks the mitochondrial targeting sequence shows a similarly mixed expression pattern (FIG 5.2E). However, when the tail of CG4567 is added to the C-terminus of CG31159, predominate nuclear localization of the protein is observed (FIG 5.2F), supporting the hypothesis that this tail can enhance nuclear localization. As expected, when the mitochondrial targeting sequence (TP) is added either to GFP or GFP-CG4567, the staining pattern dramatically changes to a predominately mitochondrial pattern (FIG 5.2G and H). No TP-GFP-CG4567 protein is visible in the nucleus of these cells (FIG 5.2H, arrow), indicating that the mitochondrial targeting sequence trumps the nuclear localization enhancement qualities of the C-terminal tail. This subcellular localization pattern likely reflects the pattern of wild-type ICO, as this GFP-tagged ICO protein can rescue *ico* mutations and so retains function. Strikingly, while GFP-tagged mutant ICO^{II032} protein (TP-GFP-CG4567-G538E) is found in the mitochondria, it is also present in the nucleus, in contrast to the wild-type ICO fusion protein (compare FIG. 5.2H and I, arrows). This altered localization pattern might be due to the *ico*^{II032} mutation affecting folding of the protein, possibly inhibiting its translocation into the mitochondria and resulting in mislocalization to the nucleus. This ectopic nuclear localization might explain why expression of ICO^{II032} proteins, but not tailless ICO^{II032}

proteins, results in the growth and patterning defects described in this chapter. It may also shed light on the issue of why missense alleles of *ico* interact with the TGF-beta screens.

Functional Rescue by Mutant Human GFM1 Proteins

In Chapter Three, the functional conservation of the fly and human *GFM1* orthologues was demonstrated by rescuing *ico* mutants with expression of transgenic human *GFM1*. Here, the functionality of two mutant GFM1 proteins identified in human patients is examined. To do this, two transgenic constructs were created to express the published human mutant GFM1 alleles *GFM1-N174S* (Coenen et al., 2004) and *GFM1-S321P* (Antonicka et al., 2006). Ubiquitous expression of either of these constructs with a combination of the *arm*- and *da-GAL4* drivers is sufficient to rescue a significant proportion of *ico* deletion mutant animals. The GFM1-N174S protein rescued 80.4% of the expected number of mutant progeny (74/92 animals), while the GFM1-S321P protein rescued 40% (38/95 animals). In both cases, the development of rescued animals was slightly delayed, with eclosion of adult flies occurring about 3-5 days later than control siblings. In contrast, expression of the mutant ICO^{II032} protein did not rescue a single animal (0/102). These striking results indicate that these two mutant human proteins still retain a significant level of functional activity in flies. However, the developmental delay seen in animals rescued with mutant human GFM1, but not wild-type human GFM1, indicates that, while functional, these mutant proteins may be less efficient or may have some moderately harmful effect that delays development.

DISCUSSION

The phenotypes of *ico* missense mutations in developing animals and in eye clones described in Chapter 4 suggest that mutant ICO proteins produced by these alleles may have toxic effects. Consistent with this hypothesis, expression of transgenic ICO^{I1032} is lethal when expressed in whole animals and has deleterious effects on growth and patterning in somatic cells in the wing. However, tailless ICO^{I1032} does not do this. These results demonstrate that in addition to loss-of-function effects, mutant ICO proteins can have harmful gain-of-function or antimorphic effects. These experiments also reveal that the C-terminal tail is necessary for the mutant protein to produce these toxic effects.

Subcellular localization experiments demonstrate that the C-terminal tail can act as a signal to enhance nuclear localization, especially when the mitochondrial targeting sequence is removed. No discernable wild-type ICO was found in the nucleus. However, it is possible that small amounts of ICO may be transported into the nucleus as part of a retrograde signaling function, similar to that of PARL (Sik, Passer, Koonin, & Pellegrini, 2004), especially under conditions in which the mitochondria are compromised. In this scenario, either the N-terminal mitochondrial targeting sequence could be cleaved off in the mitochondria, allowing the C-terminal tail to target the released protein to the nucleus, or a loss of mitochondrial membrane potential could result in decreased uptake of the protein to the mitochondria, allowing the secondary nuclear targeting signal to shunt the protein to the nucleus. Such retrograde signaling could indicate an insufficiency of competent mitochondria.

Although Antonicka et al hypothesize that perhaps a lack of stability of mutant GFM1 results in loss-of-function in human patients (Antonicka et al., 2006), these sublocalization experiments demonstrate that mutant ICO proteins are not degraded but do show ectopic nuclear localization. This suggests that mislocalization might play an important role in the pathology of GFM1 and ICO mutations. This latter hypothesis is supported by the finding that the C-terminal tail enhances ectopic nuclear localization of mutant ICO protein, and that the harmful effects of the mutant protein are attenuated with the removal of this tail. It is possible that this mislocalization of mutant ICO may result from aberrant folding of the mutant protein impeding its translocation into the mitochondria and allowing the nuclear targeting signal in the tail to redirect the protein to the nucleus. The ectopic localization of mutant protein to the nucleus could also explain why missense ico mutations interacted with screens for downstream components of the TGF-beta signaling pathway. It is possible that these mutant proteins are interacting with such components in the nucleus to affect growth and patterning. If relocation of wild-type ICO protein is used during stressful condition as a retrograde signal to indicate mitochondrial insufficiency, then it would make sense that accumulation of ICO in the nucleus could serve to negatively affect growth and proliferation (attributes which are also regulated by TGF-beta signaling).

Strikingly, rescue experiments reveal that mutant human GFM1 found in human patients retains function and can rescue *ico* mutations. However, developmental delay is seen in these rescued animals. This suggests that the either the mutant protein is not as efficient at its job or has some harmful effects as well, possibly due to mislocalization. These results are significant because they suggest that human disease

may not be caused by degradation or loss-of-function of the protein but rather by mislocalization. Why do the mutant human proteins function properly in the flies, but not in all human tissues like liver and brain? If misfolding and consequent mislocalization is an issue, perhaps the lower body temperature of flies (25C vs 37C) attenuates this aberrant folding. In human cells, it is possible that differential expression of chaperones in relatively unaffected tissues, such as the heart, may reduce misfolding of the mutant protein. It would be interesting to explore the subcellular localization of mutant human GFM1 and to examine the possible effects of temperature and chaperone expression on the location of these proteins.

Figure 5.1 Expression of mutant forms of ICO reduces growth and affects patterning in wings. (A) Heterozygous *A9-GAL4/+* female wing with wild type patterning. Longitudinal veins L1-L5 and the anterior and posterior crossveins are indicated (AC, PC). (B) Expression of a transgene encoding the mutant ICO-G538E (ICO^{I1032}) between L3 and L4 with *ptc-GAL4* driver results in reduced growth in this area and prevents the formation of the anterior crossvein (arrow). (C) Over-expression of a wild type *ico* transgene in wings using *A9-GAL4* does not affect patterning. (D) In comparison, ubiquitous expression of ICO-G538E reduces growth and interferes with proper vein formation (D). (E) Over-expression of ICO lacking the C-terminal tail has little effects on growth or patterning. (F) Unlike full-length ICO-G538E, expression of tailless ICO-G538E proteins from does not disrupt patterning.

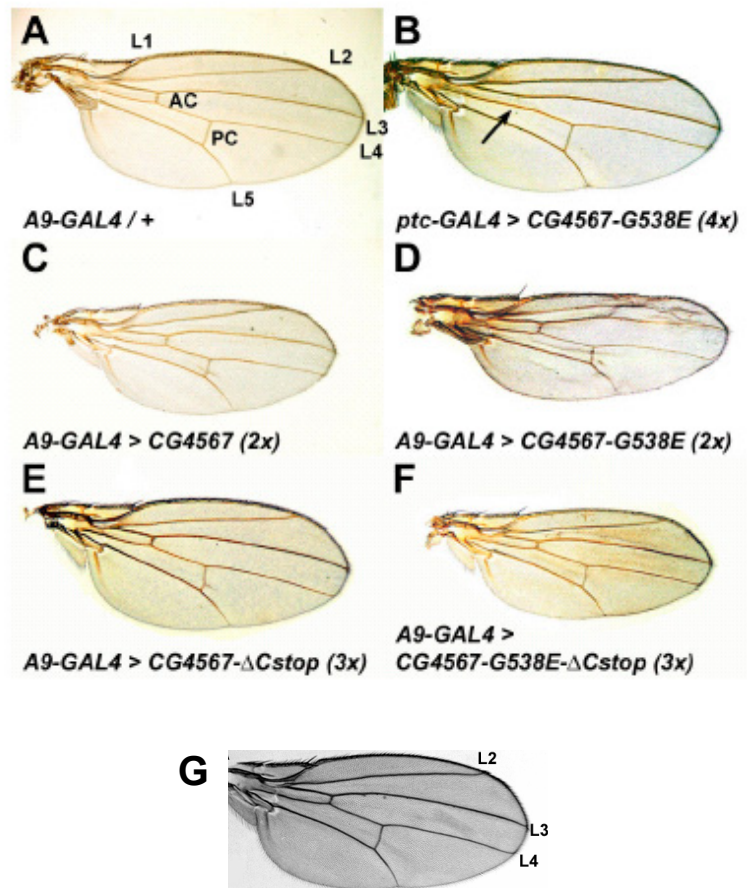


Figure 5.2 Effects of the C-terminal tail on subcellular localization of ICO proteins.

(A-I) Subcellular localization of GFP-tagged ICO (CG4567) and CG31159 proteins in living S2 cells. (A) GFP is found in the cytoplasm and the nucleus. (B) GFP-tagged ICO that lacks the N-terminal mitochondrial target sequence predominantly localizes to the nucleus. (C) Similarly, the mutant CG4567-G538E (II032) without the mitochondrial targeting sequence also mainly localizes to the nucleus. (D) In contrast, when the C-terminal tail as well as the mitochondrial targeting sequence of ICO is removed, the GFP-tagged protein is found in the cytoplasm. (E) Similarly, CG31159 without the mitochondrial targeting sequence is cytosolic and nuclear. (F) In contrast, addition of the ICO (CG4567) C-terminal tail to CG31159 changes its subcellular localization to the nucleus. (G) Addition of the N-terminal mitochondrial target protein sequence (TP) of ICO results in punctate GFP staining. (H) A similar punctate pattern is seen with a GFP-tagged wild-type ICO protein. (I) While punctate staining is also seen with the mutant CG4567-G538E, the protein is also found in the nucleus (arrow, compare to H).













	UAS-ico (<i>dGFM1</i>)	Rescue
	UAS-hGFM1	Rescue
	UAS-hGFM1 N174S	Rescue -delayed development
	UAS-hGFM1 G321P	Rescue -delayed development (40% viable)
	UAS-CG31159 (<i>dGFM2</i>)	No rescue
	UAS-CG31159+ tail	No rescue

Figure 5.3 Summary of Functional Rescue Results. Wild-type human GFM1 can rescue *ico* deletion mutants. Mutant human GFM1 can also rescue these mutants, indicating that the mutant protein still retains function. However, animals rescued with the mutant proteins show delayed development, indicating that these mutant proteins may either be less efficient or may have slightly harmful effects. CG31159 (*Drosophila* GFM2) does not rescue *ico* mutations. This suggests that adding more translation elongation factor is not sufficient to restore function and suggests that ICO may have an additional role not shared by CG31159. Addition of the C-terminal tail to CG31159 does not confer the ability to rescue *ico* mutations.

	UAS- <i>ico</i> (<i>dGFM1</i>)	Rescue
	UAS-hGFM1	Rescue
	UAS-hGFM1 N174S	Rescue -delayed development
	UAS-hGFM1 G321P	Rescue -delayed development (40% viable)
	UAS-CG31159 (<i>dGFM2</i>)	No rescue
	UAS-CG31159+ tail	No rescue

CHAPTER 6

EFFECTS OF *ICO* ON RESPONSE TO ACUTE STRESS

INTRODUCTION

As mentioned in Chapter four, heterozygous flies that have one wild-type and one mutant allele of *ico* are viable. This indicates that one normal copy of *ico* is sufficient during development. It also suggests that although mutant ICO proteins can have harmful antimorphic effects, one mutant allele is not sufficient to cause lethality. However, previous results have demonstrated that overexpression of mutant ICO in a wild-type background has deleterious effects, despite the presence of normal ICO. It is possible that the harmful effects of mutant ICO are influenced by either the amount of mutant ICO expressed or the ratio of normal to mutant ICO. In either case, it might be expected that heterozygous animals, while viable, might still demonstrate some ill effects from the single copy of either a loss-of-function deletion allele or an antimorphic missense allele. However, these heterozygotes do not appear to exhibit any defects in fecundity, longevity, or mobility. The only gross physical phenotype observed is the slightly brittle wing phenotype observed in missense mutation heterozygotes. While no significant effects are noticed under normal conditions, it is possible that these animals may exhibit phenotypes when placed under acute stress.

When a fly is exposed to certain types of acute insult, such as hyperthermia and anoxia, under which it is difficult to maintain cellular equilibrium, the animal will fall

into a protective coma (Haddad, Wyman, Mohsenin, Sun, & Krishnan, 1997). This can be observed as a failure of locomotor activity. After removal from the hyperthermic or anoxic environment, equilibrium is restored, and the animal recovers (FIG 6.1A and B). Animals that have been conditioned, such as by a prior heat-shock, are more resistant to hyperthermia and anoxia, and these animals tend to fail later and recover more quickly than non-conditioned animals (FIG 6.2A and B, data generated in the Dawson-Scully lab by C.T.). Likewise, compromised animals, such as those with mutations that affect their ability to maintain equilibrium, may fail earlier and recover later than control animals. These assays can provide important insight into the effects that a mutation may have on the flies' ability to maintain equilibrium under acute stress.

Although heterozygous flies still have a functional copy of *ico*, it is possible that having one mutant copy of the gene may attenuate the flies' ability to tolerate these types of acute stress. The following experiments were performed to determine the responses of *ico* heterozygous mutants to hyperthermic and anoxic insult.

RESULTS

Effects of *ico* Mutations on Response to Hyperthermic Insult

For these experiments, isogenized, balanced stocks of either *ico*^{H032}/CyO or *ico*^{Del EY2}/CyO were crossed out to a *yw* stock. This standard stock is often used as a control and is wild-type for the *ico* locus. The resulting *ico*^{H032}/+ and *ico*^{Del EY2}/+ progeny, along with 2-9 day old age-matched control flies, were then collected and used in the hyperthermia assay. Males and females were separated, as females tend to have a larger body size, and other factors, such as energy consumption, vary more between

females due to egg production. For this reason, the data reported here is from male flies; however, the same trends were seen in tests run with female flies.

No significant difference in failure time was observed between control flies and either of the heterozygous lines, with average failure times of between 387 and 439 seconds for all three lines (FIG 6.3A). It was interesting to note an unusual difference in the behavior of the *ico^{II032}/+* animals. While flies will climb and walk around the vial when placed in the hyperthermia chamber, *ico^{II032}/+* flies moved much more rapidly than usual, with a frenzied, jerking gait reminiscent of the behavior of the RNAi knockdown flies.

ico^{Del EY2}/+ flies showed no significant difference in recovery time from control animals (FIG 6.3 B). However, the *ico^{II032}/+* heterozygotes showed a significant ($P<0.001$) delay in recovery time, on average taking more than 55% longer (422.76 seconds vs. 272.324 seconds) to recover than wild-type controls (FIG 6.3B). This significant delay suggests while that animals with one copy of the *ico^{II032}* allele experience failure at about the same time as control animals, these mutant flies require more time to recover equilibrium after acute stress.

Effects of *ico* Mutations on Response to Anoxic Insult

As in the hyperthermia experiments, 2-9 day-old isogenized *ico^{II032}/+*, *ico^{Del EY2}/+*, and *yw* (+/+ for *ico*) male flies were used. Flies were exposed to 20 minutes of anoxia (immersion in argon gas), then were restored to the normal atmosphere and allowed to recover. Strikingly, both the *ico^{Del EY2}/+* and *ico^{II032}/+* heterozygous flies took significantly longer ($P<0.05$) to recover locomotor function than control animals

(FIG 6.4). There was no significant difference between average recovery times of *ico^{H032}/+* and *ico^{Del EY2}/+* animals.

Preliminary Studies of the Effects of *ico* Knockdown on Response to Hyperthermic and Anoxic Insult

An attempt was also made to examine the response of *ico* knockdown flies to hyperthermic insult. As described in Chapter 4, 31-33 day-old adult flies that had been expressing a *UAS-icoRNAi* construct for 26 days, as well as sibling control flies, were collected for use in the hyperthermia assay. 21/30 knockdown flies and 14/30 control flies were still alive at this relatively advanced age. Because of the limited number of flies available, the test was performed with five flies per vial instead of ten. Unfortunately, both control and knockdown flies did not recover from 650 seconds in the hyperthermia chamber at 41.5C. This is probably due to the advanced age of the flies. A second test was performed in which flies were placed in the hyperthermia chamber for 550 seconds, but, once again, none of the animals recovered. Using a time period less than 550 seconds would not be feasible, as it takes quite some time for all the flies to fail. Due to limitations resulting from the number of knockdown and control flies available, the remaining flies were saved for use in an anoxia assay. In the future, assays on knockdown flies could be performed on younger flies or at a lower temperature.

The remaining flies (11 knockdown and four control) were used in an anoxia assay. Because of the advanced age of the flies, the assay was modified so that the animals spent only 10 minutes instead of twenty under anoxic conditions. No significant difference was observed between recovery times for knockdown and control

flies (FIG). However, these results should be viewed as preliminary and interpreted with caution due to the very small sample size.

DISCUSSION

Although *ico* heterozygotes do not exhibit major phenotypes under normal conditions, these animals do show an altered response to acute stress. While *ico* heterozygotes do not exhibit differences from control animals in time to failure from hyperthermia, *ico*^{H032}/+ animals take significantly longer to recover from acute hyperthermic insult, and both missense and deletion *ico* mutants recover more slowly from anoxia. These results demonstrate that just one mutant copy of *ico* can increase sensitivity to acute stress. However, the reason for this increased sensitivity is not clear. It is possible that the increased energy demands associated with maintaining and restoring cellular equilibrium under acute stress are not as easily met in animals with only one functional copy of *ico*.

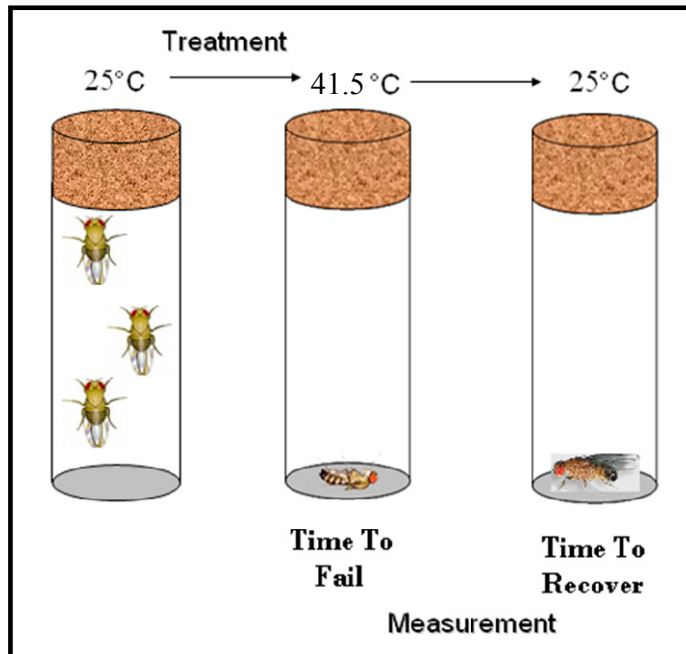
It is interesting to note that while both *ico*^{H032}/+ and *ico*^{Del EY2}/+ animals recovered more slowly from anoxia, only *ico*^{H032}/+ animals showed delayed recovery from hyperthermia. Consistent with the findings that ICO^{H032} proteins can have harmful effects, it is possible that the presence of these proteins further compromises the animal's ability to restore cellular equilibrium. This could be due to decreased capacity for energy production during stress, an increase in ROS due to inefficient functioning of the mitochondrial respiratory chain, or other, unknown causes. It would be interesting to see if *ico*^{Del EY2}/+ animals, while less sensitive than the missense mutants, might show a delay in recovery time if the temperature or time exposed to hyperthermia is

increased. Future experiments in which flies overexpressing ICO or human GFM1 proteins (wild-type or mutant) are tested in these assays would also be of interest.

Figure 6.1 Behavioral Assays. (A) Hyperthermia assay – Flies are placed in a vial in the hyperthermia chamber, and the time to failure is measured. The vial is removed to 25°C, and the time to recover locomotor activity is measured. (B) Anoxia assay – After exposure to an anoxic environment (argon gas), flies are restored to the standard atmosphere, and time to recover is measured.

A.

Hyperthermia Assay



B.

Anoxia Assay

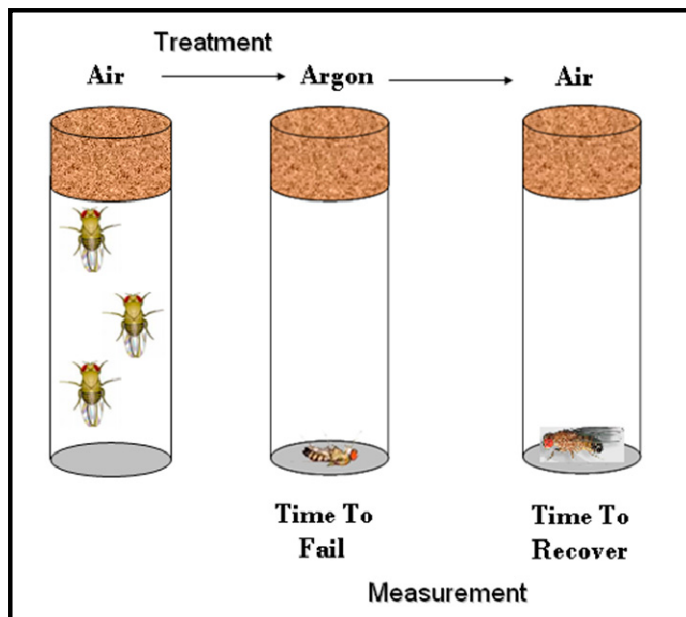
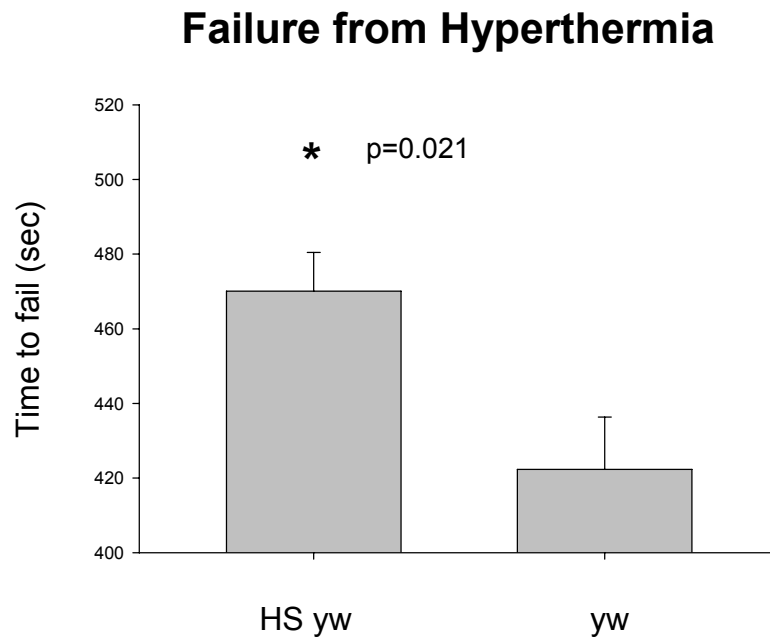


Figure 6.2 Example of disparate sensitivity to hyperthermia – the effects of heat shock on failure and recovery times. (A and B) Flies exposed to a 37C heat shock for 30 minutes and allowed to recover for one hour before placement in the hyperthermia chamber (HS) failed later and recovered more quickly than untreated control flies (yw). This demonstrates that a prior, sublethal heat shock can decrease sensitivity to hyperthermia.

A.



B.

Recovery from Hyperthermia

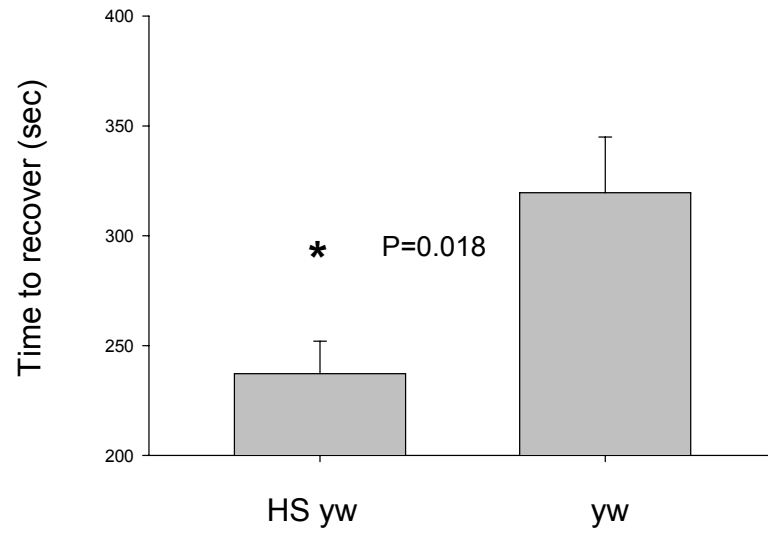
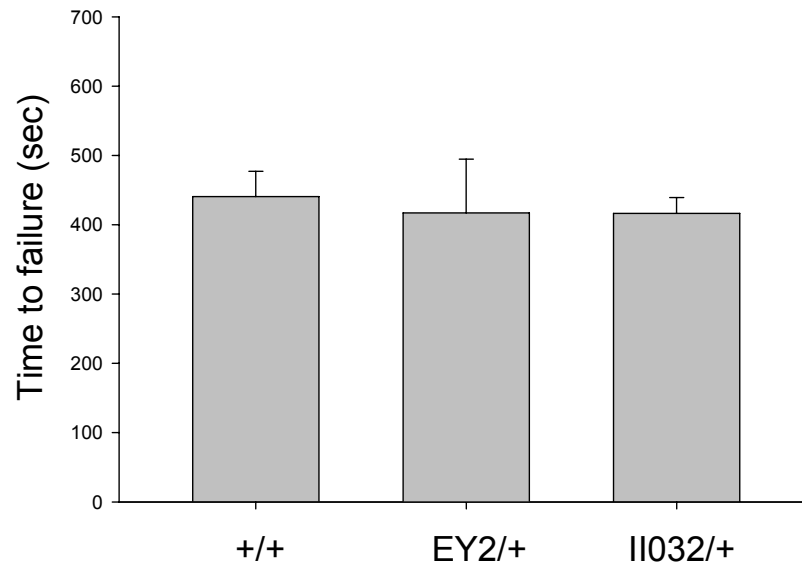


Figure 6.3 Effect of *ico* mutations on the time to failure and recovery from hyperthermia. A. Single copies of *ico* alleles do not appreciably affect the average failure time from hyperthermia insult. No significant difference in average time to failure from hyperthermia is seen between control flies (439.6 seconds) and flies heterozygous for either the *ico* deletion mutation *ico*^{Del EY2} (387.6 seconds) or the *ico* point mutation *ico*^{I1032} (417.7 seconds). B. Flies heterozygous for *ico*^{I1032} take significantly longer to recover from hyperthermia than control animals (422.8 vs. 272.3 seconds on average, respectively). In contrast, no significant difference in recovery time is seen between animals with one copy of the *ico* deletion allele *ico*^{Del EY2} and control animals.

A.

Failure from Hyperthermia



B.

Recovery from Hyperthermia

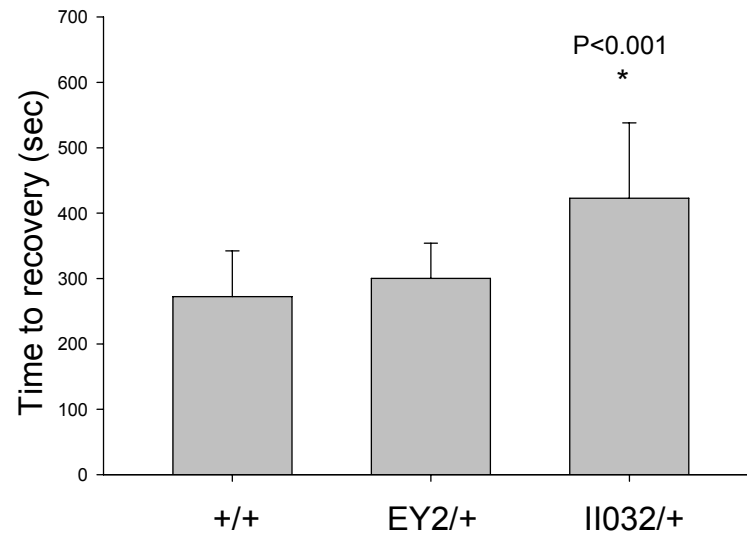


Figure 6.4 Effect of *ico* alleles on time to recover from anoxia. A single *ico* allele affects recovery from anoxia. Both *ico*^{Del EY2} deletion mutants and *ico*¹¹⁰³² point mutants recover from anoxia significantly later than control animals.

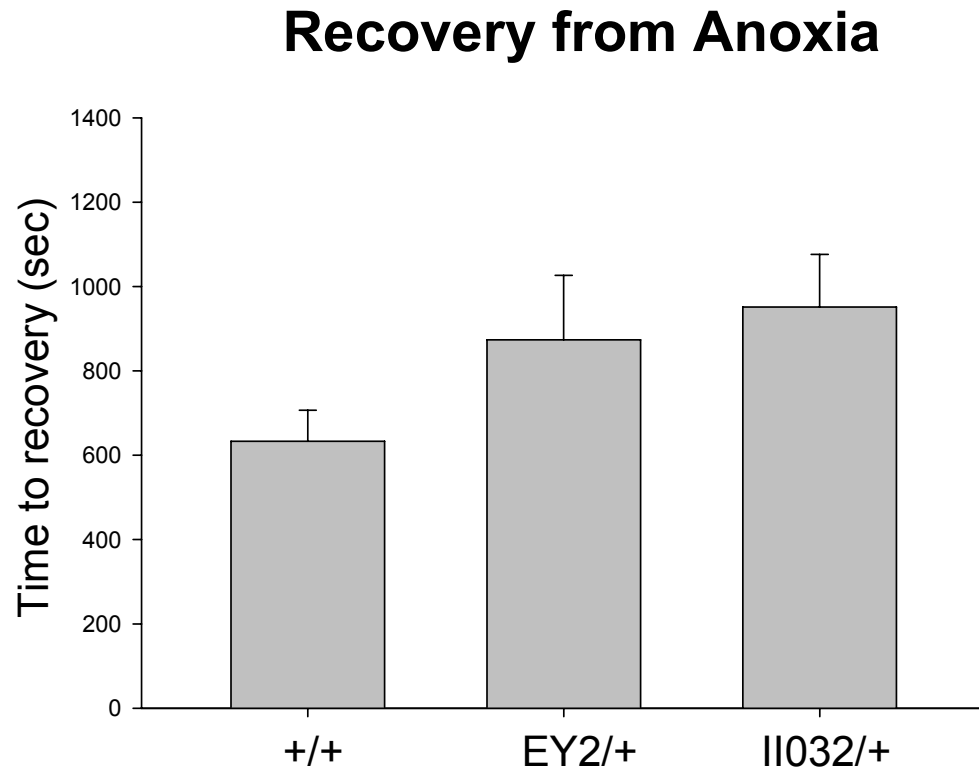
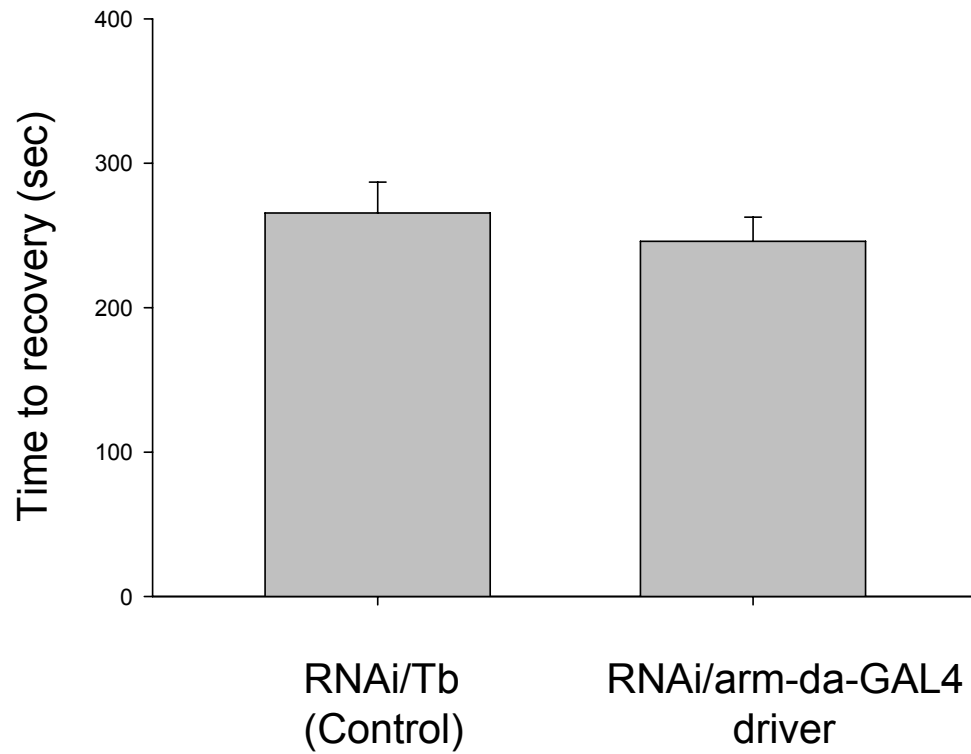


Figure 6.5 Preliminary results of *ico* knockdown animals in the anoxia assay. No significant difference was seen in recovery from anoxia between knockdown animals and controls. However, due to the small number of animals used (11 knockdown, 4 control), these results are preliminary and must be interpreted with caution.



CHAPTER 7

DISCUSSION AND FUTURE DIRECTIONS

INTRODUCTION

In this chapter, the significance of the results from the previous chapters is addressed and suggestions for future research are made.

Cloning and of *iconoclast* and Characterization of Mutations

This manuscript describes the cloning of *iconoclast*, the *Drosophila* mitochondrial translation elongation factor G1 orthologue as well as the characterization of the first known mutations in *ico*: two deletion alleles created by P-element mutagenesis, and four missense mutations that were mapped to *ico*. While both types of alleles are recessive lethal, missense mutants die earlier than deletion mutants, suggesting that mutant ICO proteins may have harmful effects in addition to possible loss-of-function consequences. Rescue experiments reveal that human GFM1 can rescue *ico* mutations, demonstrating that the human protein and fly protein are functionally conserved. In contrast, ubiquitous expression of CG31159 (fly GFM2) cannot rescue *ico* mutations, indicating that the functions of the fly GFM1 and GFM2 orthologues do not have completely overlapping functions.

Developmental Phenotypes of *ico* Mutations

The lethal phenotype of *ico* deletion mutants, which die as larvae, as well as the lethality of ubiquitous expression of *ico* RNAi during development indicates that *ico* is

an essential gene for development. However, this gene does not appear to be crucial in all adult tissues. Eye clones homozygous for *ico* deletion alleles do not exhibit defects in proliferation or patterning, and adult animals ubiquitously expressing *ico* RNAi are viable and fertile. It is possible that the second GFM protein in flies, CG31159, is sufficient to promote mitochondrial translation elongation in adult tissues. It would be interesting to use quantitative PCR to examine whether expression of CG31159 is increased in response to *ico* knockdown as well as to determine the extent of *ico* knockdown in adult animals.

The developmental lethality of *ico* deletion mutations or knockdown may be due to the reduction of available mitochondrial translation elongation factors during a time of intense energy demand. However, this hypothesis is contradicted by the finding that overexpression of CG31159 cannot rescue this lethality, indicating that increasing the amount of mitochondria translation elongation factor is not sufficient. This observation, coupled with the findings of Coenen et al that GFM2 cannot rescue the defects caused by GFM1 mutations in human fibroblasts supports the idea that GFM1 orthologues may play a role in addition to its function as a translation elongation factor.

Effects of Acute Stress on *ico* Heterozygotes

Heterozygous animals with one wild-type and one mutant *ico* allele are viable and fertile, exhibiting no major deleterious effects under normal conditions. However, these animals are more sensitive to conditions of acute stress, such as hyperthermia or anoxic insult. It is possible that these animals have difficulty coping with the large energy demands necessary to maintain and restore cellular equilibrium during these types of acute stress. To investigate this, the ability of the mitochondria in these

animals to function under acute stress can be examined. To do this, the author has developed a technique that makes use of the mitochondrial membrane potential-sensitive dye JC-1. When JC-1 interacts with polarized mitochondrial membranes, it polymerizes and fluoresces red (Cossarizza, Baccarani-Conti, Kalashnikova, & Franceschi, 1993). Loss of mitochondrial membrane potential decreases this interaction, causing the JC-1 monomers to fluoresce green. Control and heterozygous third instar larva can be filleted to expose the neuromuscular junctions (NMJ) (Brent, Werner, & McCabe, 2009). When JC-1 is introduced into the nerve at the NMJ, it can be used to examine the number of and morphology of mitochondria present, trafficking of the mitochondria along the nerve, and mitochondrial membrane potential (by determining the ratio of red-to-green fluorescence). The effects of different types of stress (such as hyperthermia or addition of hydrogen peroxide) on mitochondria in different genetic backgrounds could then be examined. While *ico* homozygous animals do not survive long enough to be used in this assay, the effects of stress on the mitochondria of heterozygous animals can be tested. The author has recently produced isogenized *ico* mutant stocks that would be appropriate for this type of assay.

Toxic Effects of Mutant ICO Proteins

In addition to possible loss-of-function consequences, mutant ICO proteins have additional antimorphic, toxic effects. *Ico* missense mutants die significantly earlier than deletion mutants. While eye clones homozygous for *ico* deletion alleles are viable, eye clones homozygous for missense mutations show patterning defects and greatly reduced proliferation. In addition, expression of transgenic mutant *ico* in developing animals is lethal, and expression in the wing results in disrupted growth and patterning. These

results are significant because this is the first indication that in addition to loss-of-function consequences, mutations in GFM1 orthologues can cause additional, antimorphic effects. The severity of these toxic effects may make it difficult to examine possible loss-of-function effects of these missense alleles. To further investigate this, the function of recombinant mutant ICO could be tested in a translation elongation assay to determine if the protein can still retain translation elongation activity.

Role of the C-terminal Tail of ICO

Unlike GFM2 orthologues or cytosolic translation elongation factors, GFM1 proteins (such as ICO) contain a positively-charged C-terminal tail. The high degree of conservation of this tail suggests that it may have an important role. Rescue experiments described in Chapter 3 demonstrate that this tail is not necessary to rescue the lethality of *ico* mutations. However, subcellular localization experiments revealed that this tail can serve to enhance nuclear localization, especially when mitochondrial translocation is impeded (by removal of the mitochondrial targeting sequence) or in mutant ICO proteins. Removal of this tail attenuates the harmful effect of mutant ICO, suggesting that the toxic effects of mutant ICO proteins is related to nuclear mislocalization of the protein. It is possible that misfolding of the mutant protein inhibits translocation into the mitochondria or otherwise enhances the ability of the protein to enter the nucleus. This nuclear mislocalization might also explain why missense mutations, but not deletion mutations, in *ico* interacted with the genetic screens for inhibition of TGF-beta signaling.

While the C-terminal tail has been shown to be crucial for the toxic effects of mutant ICO, it is unclear what its role may be in the wild-type ICO protein. Perhaps the

tail enables small amounts of ICO to act as a retrograde signal back to the nucleus. Such mitochondria-to-nucleus retrograde signaling (mediated by molecules with positively-charged peptides) has already been characterized for RIP systems, in which this signaling serves to regulate gene expression (Cao & Sudhof, 2001; Haines & Irvine, 2003), and additional roles as retrograde signaling molecules are being discovered for proteins with other known mitochondrial functions, such as PARL (Sik et al., 2004). If ICO can act in retrograde signaling, it might be expected that circumstances which limit ICO translocation into mitochondria, such as a decrease in mitochondrial membrane potential or other stress conditions, might increase the pool of protein available to be transported into the nucleus. Further sublocalization experiments to examine whether the location of wild-type ICO shifts to the nucleus when the cells are exposed to stresses such as high temperature, ROS, or compromised mitochondrial function could be helpful in investigating this issue. If the presence of ICO in the nucleus down-regulates a gene or genes involved in proliferation (which would be consistent with the observed interactions with the TGF-beta screens, as well as the overexpression experiments in which growth is disrupted), then co-immunoprecipitation assays could be useful in identifying the nuclear components that interact with ICO.

Functionality of Mutant Human GFM1

Studies in human COXPD1 patients have demonstrated that in affected tissues, such as the liver, no detectable levels of GFM1 are found in the mitochondria (Antonicka et al., 2006). In contrast, reduced but significant amounts of GFM1 are seen in the heart, which is relatively unaffected. Antonicka et al. postulate that perhaps the mutant GFM1 protein is degraded in affected tissues but is more stable in heart tissue.

Rescue experiments demonstrate that expression of human transgenic mutant GFM1 can rescue the lethality of *ico* deletion mutations, although some developmental delay is seen in rescued animals. This reveals that the mutant human proteins retain enough stability and function to enable them to compensate for the loss of endogenous ICO. However, the developmental delay observed in rescued animals suggests that the mutant protein is either less efficient or may have some additional, harmful effects. To elucidate this issue, the function of recombinant mutant GFM1 proteins in translation elongation assays could be compared with that of wild-type GFM1 to determine if a reduction in efficiency is seen with the mutant protein. Alternatively, multiple copies of transgenic mutant GFM1 could be overexpressed in the fly wing (as done in Chapter 5 with mutant ICO) to determine if it has harmful effects on growth and/or patterning.

So why do the mutant human proteins retain function in the flies, but not in all human tissues (such as the liver and the brain)? As mentioned earlier, it is possible that misfolding of the mutant proteins inhibits transport into the mitochondria, allowing the secondary targeting sequence to enhance nuclear localization. Perhaps the lower body temperature of the fly attenuates such aberrant folding and allows the mutant human proteins to efficiently enter the mitochondria. If misfolding, not instability, is the issue, this would suggest that tissue-specific differences in the type and amount of chaperone proteins expressed might influence the localization of mutant GFM1 in human patients. For example, perhaps the reason GFM1 is found in mitochondria in heart tissue, but not liver tissue, in patients is because of differentially expressed chaperones in the heart inhibiting misfolding of the mutant protein. It would be interesting to examine if significant levels of mutant GFM1 is present in the nuclei or cytoplasm of affected

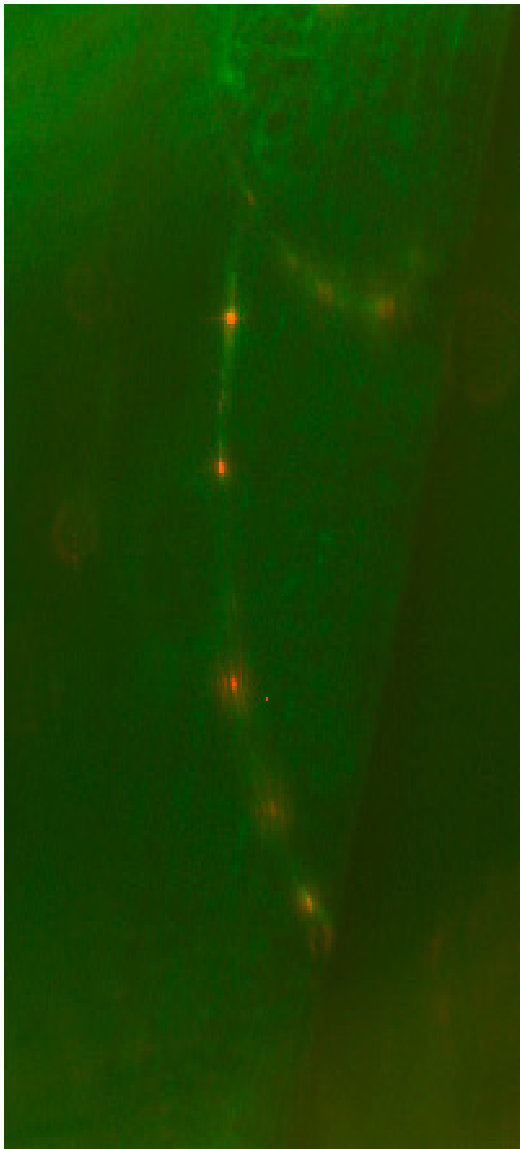
human tissues. If it is, then perhaps expression of chaperone proteins such as HSP90 or the use of chaperone-like drugs could ameliorate this mislocalization and improve OXPHOS function in these cells.

SUMMARY

These experiments describe the identification and characterization of the first mutations in *iconoclast*, the fly mitochondrial translation elongation factor G1. These results demonstrate that in addition to loss-of-function consequences, mutations in *ico* can produce proteins with toxic antimorphic effects on growth and patterning. The positively-charged C-terminal tail of ICO has been shown to enhance ectopic nuclear localization of mutant ICO and is necessary for the harmful effects of the mutant protein.

The data presented here may have important implications for understanding the pathology underlying human disease caused by GFM1 mutations. Mutant versions of the human protein, GFM1, can rescue *ico* mutations, indicating that the proteins still retain function. Taken together with the subcellular localization data, these results support the hypothesis that mislocalization, not instability or loss-of-function, of mutant GFM1 may be responsible for the pathology seen in affected human tissues. In addition to loss-of-function consequences, it is also possible that mutant human GFM1 can have antimorphic effects like ICO. Further work is needed to examine these issues.

Figure 7.1. JC-1 staining in the fly neuromuscular junction. JC-1 fluoresces red when it interacts with polarized mitochondrial membranes of competent mitochondria. The number, morphology, and movement of the mitochondria can be tracked in live nerves by perfusing this dye into a larval neuromuscular junction preparation. In addition, the ratio of red to green fluorescence is indicative of the mitochondrial membrane potential.



REFERENCES

- Anderson, S., Bankier, A. T., Barrell, B. G., de Bruijn, M. H., Coulson, A. R., Drouin, J., et al. (1981). Sequence and organization of the human mitochondrial genome. *Nature*, 290(5806), 457-465.
- Antonicka, H., Sasarman, F., Kennaway, N. G., & Shoubridge, E. A. (2006). The molecular basis for tissue specificity of the oxidative phosphorylation deficiencies in patients with mutations in the mitochondrial translation factor EFG1. *Hum Mol Genet*, 15(11), 1835-1846.
- Baker, K. D., & Thummel, C. S. (2007). Diabetic larvae and obese flies-emerging studies of metabolism in *Drosophila*. *Cell Metab*, 6(4), 257-266.
- Bellance, N., Lestienne, P., & Rossignol, R. (2009). Mitochondria: from bioenergetics to the metabolic regulation of carcinogenesis. *Front Biosci*, 14, 4015-4034.
- Bernards, A., & Hariharan, I. K. (2001). Of flies and men--studying human disease in *Drosophila*. *Curr Opin Genet Dev*, 11(3), 274-278.
- Bier, E. (2005). *Drosophila*, the golden bug, emerges as a tool for human genetics. *Nat Rev Genet*, 6(1), 9-23.
- Brand, A. H., & Perrimon, N. (1993). Targeted gene expression as a means of altering cell fates and generating dominant phenotypes. *Development*, 118(2), 401-415.
- Brent, J. R., Werner, K. M., & McCabe, B. D. (2009). *Drosophila* larval NMJ dissection. *J Vis Exp*(24).

- Brown, N. H., & Kafatos, F. C. (1988). Functional cDNA libraries from *Drosophila* embryos. *J Mol Biol*, 203(2), 425-437.
- Cain, K., & Freathy, C. (2001). Liver toxicity and apoptosis: role of TGF-beta1, cytochrome c and the apoptosome. *Toxicol Lett*, 120(1-3), 307-315.
- Cao, X., & Sudhof, T. C. (2001). A transcriptionally [correction of transcriptively] active complex of APP with Fe65 and histone acetyltransferase Tip60. *Science*, 293(5527), 115-120.
- Celniker, S. E., & Rubin, G. M. (2003). The *Drosophila melanogaster* genome. *Annu Rev Genomics Hum Genet*, 4, 89-117.
- Coenen, M. J., Antonicka, H., Ugalde, C., Sasarman, F., Rossi, R., Heister, J. G., et al. (2004). Mutant mitochondrial elongation factor G1 and combined oxidative phosphorylation deficiency. *N Engl J Med*, 351(20), 2080-2086.
- Cossarizza, A., Baccarani-Contrì, M., Kalashnikova, G., & Franceschi, C. (1993). A new method for the cytofluorimetric analysis of mitochondrial membrane potential using the J-aggregate forming lipophilic cation 5,5',6,6'-tetrachloro-1,1',3,3'-tetraethylbenzimidazolcarbocyanine iodide (JC-1). *Biochem Biophys Res Commun*, 197(1), 40-45.
- Duffy, J. B. (2002). GAL4 system in *Drosophila*: a fly geneticist's Swiss army knife. *Genesis*, 34(1-2), 1-15.
- Feany, M. B., & Bender, W. W. (2000). A *Drosophila* model of Parkinson's disease. *Nature*, 404(6776), 394-398.

- Gao, J., Yu, L., Zhang, P., Jiang, J., Chen, J., Peng, J., et al. (2001). Cloning and characterization of human and mouse mitochondrial elongation factor G, GFM and Gfm, and mapping of GFM to human chromosome 3q25.1-q26.2. *Genomics*, 74(1), 109-114.
- Haddad, G. G., Wyman, R. J., Mohsenin, A., Sun, Y., & Krishnan, S. N. (1997). Behavioral and Electrophysiologic Responses of *Drosophila melanogaster* to Prolonged Periods of Anoxia. *J Insect Physiol*, 43(3), 203-210.
- Haines, N., & Irvine, K. D. (2003). Glycosylation regulates Notch signalling. *Nat Rev Mol Cell Biol*, 4(10), 786-797.
- Hammarsund, M., Wilson, W., Corcoran, M., Merup, M., Einhorn, S., Grander, D., et al. (2001). Identification and characterization of two novel human mitochondrial elongation factor genes, hEFG2 and hEFG1, phylogenetically conserved through evolution. *Hum Genet*, 109(5), 542-550.
- Haywood, A. F., & Staveley, B. E. (2006). Mutant alpha-synuclein-induced degeneration is reduced by parkin in a fly model of Parkinson's disease. *Genome*, 49(5), 505-510.
- Hoodless, P. A., Haerry, T., Abdollah, S., Stapleton, M., O'Connor, M. B., Attisano, L., et al. (1996). MADR1, a MAD-related protein that functions in BMP2 signaling pathways. *Cell*, 85(4), 489-500.
- Huang, S. L., & Baker, B. S. (1976). The mutability of the minute loci of *Drosophila melanogaster* with ethyl methanesulfonate. *Mutat Res*, 34(3), 407-414.

- Jackson, G. R., Salecker, I., Dong, X., Yao, X., Arnheim, N., Faber, P. W., et al. (1998). Polyglutamine-expanded human huntingtin transgenes induce degeneration of *Drosophila* photoreceptor neurons. *Neuron*, 21(3), 633-642.
- Jacobs, H. T. (2003). Disorders of mitochondrial protein synthesis. *Hum Mol Genet*, 12 Spec No 2, R293-301.
- Jacobs, H. T., & Turnbull, D. M. (2005). Nuclear genes and mitochondrial translation: a new class of genetic disease. *Trends Genet*, 21(6), 312-314.
- Koc, E. C., & Spremulli, L. L. (2002). Identification of mammalian mitochondrial translational initiation factor 3 and examination of its role in initiation complex formation with natural mRNAs. *J Biol Chem*, 277(38), 35541-35549.
- Konopka, R. J., & Benzer, S. (1971). Clock mutants of *Drosophila melanogaster*. *Proc Natl Acad Sci U S A*, 68(9), 2112-2116.
- Lazzaro, B. P., & Galac, M. R. (2006). Disease pathology: wasting energy fighting infection. *Curr Biol*, 16(22), R964-965.
- Lewis, E. B. (1941). Another Case of Unequal Crossing-Over in *Drosophila Melanogaster*. *Proc Natl Acad Sci U S A*, 27(1), 31-35.
- Lewis, E. B. (1945). The Relation of Repeats to Position Effect in *Drosophila Melanogaster*. *Genetics*, 30(2), 137-166.
- Lewis, E. B. (1948). Pseudoallelism in *Drosophila melanogaster*. *Genetics*, 33(1), 113.
- Lewis, E. B. (1952). The Pseudoallelism of White and Apricot in *Drosophila Melanogaster*. *Proc Natl Acad Sci U S A*, 38(11), 953-961.
- Lewis, E. B. (1978). A gene complex controlling segmentation in *Drosophila*. *Nature*, 276(5688), 565-570.

- Lewis, E. B. (1982). Control of body segment differentiation in *Drosophila* by the bithorax gene complex. *Prog Clin Biol Res*, 85 Pt A, 269-288.
- Ling, M., Merante, F., Chen, H. S., Duff, C., Duncan, A. M., & Robinson, B. H. (1997). The human mitochondrial elongation factor tu (EF-Tu) gene: cDNA sequence, genomic localization, genomic structure, and identification of a pseudogene. *Gene*, 197(1-2), 325-336.
- Luong, N., Davies, C. R., Wessells, R. J., Graham, S. M., King, M. T., Veech, R., et al. (2006). Activated FOXO-mediated insulin resistance is blocked by reduction of TOR activity. *Cell Metab*, 4(2), 133-142.
- Ma, J., Farwell, M. A., Burkhart, W. A., & Spremulli, L. L. (1995). Cloning and sequence analysis of the cDNA for bovine mitochondrial translational initiation factor 2. *Biochim Biophys Acta*, 1261(2), 321-324.
- Ma, J., & Ptashne, M. (1987). A new class of yeast transcriptional activators. *Cell*, 51(1), 113-119.
- Milne, J. C., Lambert, P. D., Schenk, S., Carney, D. P., Smith, J. J., Gagne, D. J., et al. (2007). Small molecule activators of SIRT1 as therapeutics for the treatment of type 2 diabetes. *Nature*, 450(7170), 712-716.
- Muller, H. J. (1928). The Measurement of Gene Mutation Rate in *Drosophila*, Its High Variability, and Its Dependence upon Temperature. *Genetics*, 13(4), 279-357.
- Myers, A. M., Pape, L. K., & Tzagoloff, A. (1985). Mitochondrial protein synthesis is required for maintenance of intact mitochondrial genomes in *Saccharomyces cerevisiae*. *Embo J*, 4(8), 2087-2092.

- Nichols, C. D. (2006). *Drosophila melanogaster* neurobiology, neuropharmacology, and how the fly can inform central nervous system drug discovery. *Pharmacol Ther*, 112(3), 677-700.
- Nüsslein-Volhard, C., E. W., & H., K. (1984). Mutations affecting the pattern of the larval cuticle in *Drosophila melanogaster*. I. Zygotic loci on the second chromosome. *Roux's Archives in Developmental Biology*, 193, 267-282.
- Pieper, U., Eswar, N., Braberg, H., Madhusudhan, M. S., Davis, F. P., Stuart, A. C., et al. (2004). MODBASE, a database of annotated comparative protein structure models, and associated resources. *Nucleic Acids Res*, 32(Database issue), D217-222.
- Preston, C. R., Sved, J. A., & Engels, W. R. (1996). Flanking duplications and deletions associated with P-induced male recombination in *Drosophila*. *Genetics*, 144(4), 1623-1638.
- Rafferty, L. A., Twombly, V., Wharton, K., & Gelbart, W. M. (1995). Genetic screens to identify elements of the decapentaplegic signaling pathway in *Drosophila*. *Genetics*, 139(1), 241-254.
- Ravikumar, B., Vacher, C., Berger, Z., Davies, J. E., Luo, S., Oroz, L. G., et al. (2004). Inhibition of mTOR induces autophagy and reduces toxicity of polyglutamine expansions in fly and mouse models of Huntington disease. *Nat Genet*, 36(6), 585-595.
- Robertson, H. M., Preston, C. R., Phillis, R. W., Johnson-Schlitz, D. M., Benz, W. K., & Engels, W. R. (1988). A stable genomic source of P element transposase in *Drosophila melanogaster*. *Genetics*, 118(3), 461-470.

- Romero, M. F., Henry, D., Nelson, S., Harte, P. J., Dillon, A. K., & Sciortino, C. M. (2000). Cloning and characterization of a Na⁺-driven anion exchanger (NDAE1). A new bicarbonate transporter. *J Biol Chem*, 275(32), 24552-24559.
- Rooke, H. M., & Crosier, K. E. (2001). The smad proteins and TGFbeta signalling: uncovering a pathway critical in cancer. *Pathology*, 33(1), 73-84.
- Rubio-Gozalbo, M. E., Dijkman, K. P., van den Heuvel, L. P., Sengers, R. C., Wendel, U., & Smeitink, J. A. (2000). Clinical differences in patients with mitochondriocytopathies due to nuclear versus mitochondrial DNA mutations. *Hum Mutat*, 15(6), 522-532.
- Sasarman, F., Antonicka, H., & Shoubridge, E. A. (2008). The A3243G tRNA^{Leu}(UUR) MELAS mutation causes amino acid misincorporation and a combined respiratory chain assembly defect partially suppressed by overexpression of EFTu and EFG2. *Hum Mol Genet*, 17(23), 3697-3707.
- Schapira, A. H. (2006). Mitochondrial disease. *Lancet*, 368(9529), 70-82.
- Scherzer, C. R., Jensen, R. V., Gullans, S. R., & Feany, M. B. (2003). Gene expression changes presage neurodegeneration in a Drosophila model of Parkinson's disease. *Hum Mol Genet*, 12(19), 2457-2466.
- Sciortino, C. M., Shrode, L. D., Fletcher, B. R., Harte, P. J., & Romero, M. F. (2001). Localization of endogenous and recombinant Na⁽⁺⁾-driven anion exchanger protein NDAE1 from Drosophila melanogaster. *Am J Physiol Cell Physiol*, 281(2), C449-463.

- Sik, A., Passer, B. J., Koonin, E. V., & Pellegrini, L. (2004). Self-regulated cleavage of the mitochondrial intramembrane-cleaving protease PARL yields Pbeta, a nuclear-targeted peptide. *J Biol Chem*, 279(15), 15323-15329.
- Stowers, R. S., & Schwarz, T. L. (1999). A genetic method for generating *Drosophila* eyes composed exclusively of mitotic clones of a single genotype. *Genetics*, 152(4), 1631-1639.
- Sturtevant, A. H., Bridges, C. B., & Morgan, T. H. (1919). The Spatial Relations of Genes. *Proc Natl Acad Sci U S A*, 5(5), 168-173.
- Thorburn, D. R. (2004). Mitochondrial disorders: prevalence, myths and advances. *J Inherit Metab Dis*, 27(3), 349-362.
- Tickoo, S., & Russell, S. (2002). *Drosophila melanogaster* as a model system for drug discovery and pathway screening. *Curr Opin Pharmacol*, 2(5), 555-560.
- Tiong, S. Y., & Nash, D. (1990). Genetic analysis of the adenosine3 (Gart) region of the second chromosome of *Drosophila melanogaster*. *Genetics*, 124(4), 889-897.
- Tsuboi, M., Morita, H., Nozaki, Y., Akama, K., Ueda, T., Ito, K., et al. (2009). EF-G2mt is an exclusive recycling factor in mammalian mitochondrial protein synthesis. *Mol Cell*, 35(4), 502-510.
- Valente, L., Tiranti, V., Marsano, R. M., Malfatti, E., Fernandez-Vizarra, E., Donnini, C., et al. (2007). Infantile encephalopathy and defective mitochondrial DNA translation in patients with mutations of mitochondrial elongation factors EFG1 and EFTu. *Am J Hum Genet*, 80(1), 44-58.

- Vambutas, A., Ackerman, S. H., & Tzagoloff, A. (1991). Mitochondrial translational-initiation and elongation factors in *Saccharomyces cerevisiae*. *Eur J Biochem*, 201(3), 643-652.
- Wang, Y., & Gu, X. (2000). Evolutionary patterns of gene families generated in the early stage of vertebrates. *J Mol Evol*, 51(1), 88-96.
- Woriak, V. L., Burkhardt, W., & Spremulli, L. L. (1995). Cloning, sequence analysis and expression of mammalian mitochondrial protein synthesis elongation factor Tu. *Biochim Biophys Acta*, 1264(3), 347-356.
- Xin, H., Woriak, V., Burkhardt, W., & Spremulli, L. L. (1995). Cloning and expression of mitochondrial translational elongation factor Ts from bovine and human liver. *J Biol Chem*, 270(29), 17243-17249.
- Zhang, Y., & Spremulli, L. L. (1998). Identification and cloning of human mitochondrial translational release factor 1 and the ribosome recycling factor. *Biochim Biophys Acta*, 1443(1-2), 245-250.
- Zhou, D., Xue, J., Lai, J. C., Schork, N. J., White, K. P., & Haddad, G. G. (2008). Mechanisms underlying hypoxia tolerance in *Drosophila melanogaster*: hairy as a metabolic switch. *PLoS Genet*, 4(10), e1000221.